

THESIS FOR THE DEGREE OF DOCTOR OF PHILOSOPHY

Engineering Cytosolic Acetyl-CoA Metabolism in *Saccharomyces cerevisiae*

Combining metabolic engineering and adaptive laboratory evolution

YIMING ZHANG



Department of Biology and Biological Engineering
CHALMERS UNIVERSITY OF TECHNOLOGY
Gothenburg, Sweden 2015

Engineering Cytosolic Acetyl-CoA Metabolism in *Saccharomyces cerevisiae*

Combining metabolic engineering and adaptive laboratory evolution

YIMING ZHANG

@YIMING ZHANG, 2015

ISBN: 978-91-7597-147-6

Doktorsavhandlingar vid Chalmers tekniska högskola

Ny serie nr: 3828

ISSN: ISSN 0346-718X

Systems and Synthetic Biology Group
Department of Biology and Biological Engineering
Chalmers University of Technology
SE-412 96 Göteborg
Sweden
Telephone +46 (0) 31-772 1000

Cover illustration:

A simple illustration for possible roles of the mutated proteins in the evolved Pdc negative strains.
For more details, refer to Figure 14B.

Printed by Chalmers Reproservice

Göteborg, Sweden 2015

PREFACE

This dissertation serves as a partial fulfilment of the requirement to obtain the degree of doctor of philosophy at Department of Biology and Biological Engineering, Chalmers University of Technology, Sweden. The research was carried out in Systems and Synthetic Biology group under the supervision of Professor Jens Nielsen. This study combines metabolic engineering and adaptive laboratory evolution to establish a non-ethanol producing yeast strain as a cell factory. The research was funded by the doctoral scholarship program of China Scholarship Council (China), the Chalmers Foundation, Vetenskapsrådet, FORMAS and European Research Council (Grant no. 247013).

Yiming Zhang

January 2015

Abstract

A *Saccharomyces cerevisiae* strain carrying deletions in all three pyruvate decarboxylase genes (also called Pdc negative yeast) represents a non-ethanol producing platform strain for biochemical production. However, it cannot grow on glucose as the sole carbon source due to the lack of cytosolic acetyl-CoA for lipid biosynthesis. Its growth inability on glucose could be restored through directed evolution, which was explained by an in-frame internal deletion in *MTH1* (*MTH1-ΔT*). The *MTH1-ΔT* allele resulted in reduced glucose uptake, which may attenuate the repression of respiratory metabolism. However, it was not clear what mechanism could provide the cells with sufficient precursors for cytosolic acetyl-CoA. Here we investigated this using a Pdc negative strain with *MTH1-ΔT*, IMI076. Our results identified a route relying on Ach1 that could transfer acetyl units from mitochondria to the cytoplasm. Based on the results a new model was proposed, in which acetyl units are shuttled from the mitochondria to the cytoplasm in the form of acetate. In addition, a collection of Pdc negative strains was constructed and one of them was adaptively evolved on glucose via serial transfer. Three independently evolved strains were obtained, which can grow on glucose as the sole carbon source at maximum specific rates of 0.138 h^{-1} , 0.148 h^{-1} , 0.141 h^{-1} , respectively. Several genetic changes were identified in the evolved Pdc negative strains by genome sequencing. Among these genetic changes, 4 genes were found to carry point mutations in at least two of the evolved strains: *MTH1*, *HXT2*, *CIT1*, and *RPD3*. Reverse engineering of the non-evolved Pdc negative strain through introduction of the *MTH1*^{81D} allele restored its growth on glucose at a maximum specific rate of 0.05 h^{-1} in minimal medium with 2% glucose. The non-synonymous mutations in *HXT2* and *CIT1* may function in the presence of mutated *MTH1* alleles and could be related to an altered central carbon metabolism in order to ensure production of cytosolic acetyl-CoA in the Pdc negative strain.

In connection with biobased chemical production, it is necessary to engineer the metabolism of cell factories such that the raw material, typically sugars, can be efficiently converted to the product of interest. Although IMI076 could grow on glucose, it was still inefficient at conversion of pyruvate to cytosolic acetyl-CoA. To increase cytosolic acetyl-CoA supply from pyruvate, pyruvate formate lyase and its activating enzyme from *Escherichia coli* were expressed with two different cofactors, ferredoxin or flavodoxin, and their reductase, respectively, and it was found that the co-expression of either of these cofactors had a positive effect on growth under aerobic conditions, indicating increased activity of PFL. The positive effect on growth was manifested as a higher final biomass concentration and a significant increase in transcription of formate dehydrogenase genes (*FDHs*). Among the two cofactors reduced flavodoxin was found to be a better electron donor than reduced ferredoxin.

Key words: yeast, acetyl-CoA, central carbon metabolism, mitochondria, pyruvate decarboxylase, genomic DNA sequencing, reverse engineering, adaptive evolution, hexose transporter, citrate synthase, histone deacetylase; ferredoxin, flavodoxin, ferredoxin/flavodoxin NADP⁺ reductase, aerobic growth, metabolic engineering.

LIST OF PUBLICATIONS

The thesis is based on the following publications, referred to as Paper I to IV in the text:

- I. Ach1 is involved in shuttling mitochondrial acetyl units for cytosolic C2 provision in Pdc negative *Saccharomyces cerevisiae***
Yun Chen*, Yiming Zhang*, Verena Siewers, Jens Nielsen.
Submitted for publication.
- II. Adaptive mutations in sugar metabolism restore growth on glucose in a pyruvate decarboxylase negative yeast strain**
Yiming Zhang, Martin KM Engqvist, Anastasia Krivoruchko, Björn M Hallström, Yun Chen, Verena Siewers, Jens Nielsen.
Submitted for publication.
- III. Functional pyruvate formate lyase pathway expressed with its cofactors in *Saccharomyces cerevisiae* at aerobic growth**
Yiming Zhang, Anastasia Krivoruchko, Yun Chen, Verena Siewers, Jens Nielsen.
Submitted for publication.
- IV. Microbial acetyl-CoA metabolism and metabolic engineering (Review)**
Anastasia Krivoruchko, Yiming Zhang, Verena Siewers, Yun Chen, Jens Nielsen.
Metabolic Engineering, March 2015; 28: 28–42.

* Equal contribution

Additional publications during doctoral research not included in this thesis:

- V. Improving heterologous protein secretion in aerobic conditions by activating hypoxia induced genes in *Saccharomyces cerevisiae***
Lifang Liu, Yiming Zhang, Zihé Liu, Verena Siewers, Dina Petranovic, Jens Nielsen.
Submitted for publication.

CONTRIBUTION TO MANUSCRIPTS

A summary of my contribution to each of the publications listed is provided below:

- I. Designed research; performed the research; analyzed the data; assisted in the manuscript preparation.
- II. Designed research; performed the research; analyzed the data; wrote the manuscript.
- III. Designed research; performed the research; analyzed the data; wrote the manuscript.
- IV. Assisted in the manuscript preparation.
- V. Designed and performed part of the research; analyzed the data; assisted in the manuscript preparation.

LIST OF FIGURES AND TABLES

Figure 1. Overview of acetyl-CoA metabolism in yeast (Adapted from [6]).	3
Figure 2. Addition of succinate improves the growth of the strain IMI076	19
Figure 3. The growth of the strain IMI076 (<i>Pdc⁻ MTH1-ΔT</i>) relies on Ach1.	20
Figure 4. Complementation with the intact <i>ACH1</i> but not the truncated version restores growth of an <i>ach1</i> mutant.	21
Figure 5. Growth assays of IMI076 (A) and CEN.PK 113-5D (B) upon addition of UK-5099	22
Figure 6. A model of Ach1 transferring acetyl units from the mitochondria to the cytosol	23
Figure 7. Bipartite strategy for gene deletion.	24
Figure 8. Work flow of Pdc negative strain construction.	25
Figure 9. Adaptive evolution process of the Pdc negative strain E1.	25
Figure 10. Reverse engineering strategy for <i>MTH1^{81D}</i> integration into <i>MTH1</i> locus of the E1 strain	28
Figure 11. Growth profiles of reverse engineered strains M81-11 and M81-33 (two transformants, <i>ura3-52 his3-Δ1 pdc1Δ pdc5Δ pdc6Δ mth1::MTH1^{81D}</i>) in minimal medium with 2% glucose. All measurements are mean +/- standard error of three biological replicates.	29
Figure 12. Transcription analysis of <i>HXTs</i> (<i>HXT1-7</i>) in two M81 strains and wild type strain CEN.PK 113-11C.	30
Figure 13. Mapping and analysis of mutations in Mth1 (A), Hxt2 (B), Cit1 (C) and Rpd3 (D).	31
Figure 14. A cartoon representation of homology protein models generated for Hxt2 (A), Cit1 (B) and Rpd3 (C)	32
Figure 15. Predictions on the secondary structure of Mth1 protein	33
Figure 16. A simple illustration for the possible roles of the mutated proteins in the evolved pdc negative strains	36
Figure 17. Growth comparisons of the strains with and without the PFL pathway	38
Figure 18. Growth comparisons of YZ10, YZ11, YZ12 and YZ13 in minimal medium using shake flasks	39
Figure 19 Expression analysis of introduced genes in YZ12 (A) and YZ13 (B)	40
Figure 20. Expression analysis of <i>FDH1</i> and <i>FDH2</i> in YZ10-1, YZ11-1, YZ13-2 and YZ13-6.	41
Table 1. Point mutations in evolved Pdc negative strains.	27
Table 2. Strain properties of YZ10, YZ11, YZ12 and YZ13.	39

ABBREVIATIONS AND SYMBOLS

TCA: tricarboxylic acid

GYC: glyoxylate cycle

μ_{\max} : maximum specific growth rate

Y_{Pyr} : pyruvate yield on glucose as the substrate

Y_{Gly} : glycerol yield on glucose as the substrate

Chr: chromosome

Yeast nomenclature

Gene name consist of three letters and up to three numbers in italic, *e.g. PDC1, acs1*;

Wild type gene name is written with upper letters in italic, *e.g. PDC1, ACS1*;

Recessive gene name is written with lower letters in italic, *e.g. pdc1, acs1*;

Mutant alleles are named with a dash and a number in italic, *e.g. ura3-52*;

Deleted gene with the genetic marker used for deletion, *e.g. pdc1 Δ , pdc1::loxP*;

The protein product of the gene is written with an upper letter at the first letter and two lower letters in normal font, *e.g. Pdc1, Acs1*;

Exception case for gene name: *MATa, MAT α , MTH1- ΔT* ;

Genes with amino acid sequence change is written with gene name and changed amino acid with its position, *e.g. MTH1^{81D}*.

TABLE OF CONTENTS

PREFACE	iii
Abstract	iv
LIST OF PUBLICATIONS	v
CONTRIBUTION TO MANUSCRIPTS.....	vi
LIST OF FIGURES AND TABLES	vii
ABBREVIATIONS AND SYMBOLS	viii
TABLE OF CONTENTS	ix
Chapter 1 Introduction	1
1 Yeast <i>Saccharomyces cerevisiae</i> as a cell factory	1
1.1 Acetyl-CoA metabolism in yeast	3
1.1.1 Acetyl-CoA use in the TCA cycle and glyoxylate cycle	3
1.1.2 Acetyl-CoA use in the PDH bypass.....	6
1.1.3 Acetyl-CoA use in fatty acid and sterol metabolism	8
1.1.4 Acetyl-CoA transport between subcellular organelles	8
1.1.5 Acetyl-CoA in protein acetylation	9
1.2 Non-ethanol producing strain for biochemical production	10
1.2.1 Pyruvate decarboxylase	10
1.2.2 Pyruvate decarboxylase negative strain	11
1.3 Metabolic engineering and adaptive evolution in strain development.....	13
Chapter 2. Overview of the thesis	15
Chapter 3. Results and discussion	18
3.1 ACH1 compensates cytosolic acetyl-CoA in Pdc negative strain.....	18
3.2 Growth recovery through adaptive evolution and reverse metabolic engineering.....	24
3.3 Functional bacterial pyruvate formate lyase expressed in pdc negative strain	37
Chapter 4. Conclusions and perspective	42
Acknowledgments.....	44
References	45

Chapter 1 Introduction

1 Yeast *Saccharomyces cerevisiae* as a cell factory

The yeast *Saccharomyces cerevisiae* (also called budding yeast, Brewer's yeast, or Baker's yeast, referred to as yeast in this thesis except when otherwise specified) has been used in food and beverage fermentation by human beings since ancient times. As an important model microorganism for eukaryotes, yeast has been intensively studied in molecular and cell biology, genetics and systems biology, much like *Escherichia coli* as the model for prokaryotes. Due to its robustness and tolerance towards industrial conditions, as well as its Generally Regarded As Safe (GRAS) feature, yeast has been exploited as an important cell factory for industrial production of chemical compounds [1]. With the development of metabolic engineering and synthetic biology [2], yeast is already used for production of various bio-compounds, ranging from large volume fermentation products, like bioethanol, big volume fermentation products like succinic acid, to small volume fermentation product of several pharmaceuticals, like human insulin [3, 4].

With the requirements for sustainable solutions to provide fuels, chemicals and pharmaceuticals, now there is increasing focus on cell factories, as they may serve as one of the pillars underlying a sustainable society [5]. As a very important cell factory already widely used for production of biofuels, chemicals and pharmaceuticals, there is much interest in developing platform strains of yeast that can be used for production of a whole range of different products.

Yeast can efficiently convert the raw material into precursor metabolites, and these precursor metabolites are then further converted into the products of interest. One of these precursor metabolites is **acetyl-CoA**, which used as precursor for the production of a wide range of valuable products, like 1-butanol, polyhydroxybutyrates, isoprenoids, polyketides, alkanes, alkenes, fatty alcohols and waxes etc.[6]. Most of these products are produced from synthetic pathways that are reconstructed and generally positioned in the cytosol as this will minimize secretion issues of the bio-products. In previous studies, it has been suggested that cytosolic acetyl-CoA availability is a limiting factor for bio-compound production probably due to the low activity and high-energy input requirements of the acetyl-CoA synthetase in yeast. Different successful strategies have been performed and evaluated to increase the production of several bio-compounds by enhancing cytosolic acetyl-CoA supply [7].

In yeast, acetyl-CoA metabolism (as described in Chapter 1.1) is highly compartmentalized and it cannot be transported across different subcellular organelles

readily. Cytosolic acetyl-CoA is generated via the pyruvate dehydrogenase (PDH) bypass, which involves three enzymes, pyruvate decarboxylase (PDC), acetaldehyde dehydrogenase (ALD) and acetyl-CoA synthetase (ACS). By over-expressing the native acetaldehyde dehydrogenase gene *ALD6* and a mutant acetyl-CoA synthetase gene *ACS_{SE}^{L641P}*, the production of amorphadiene increased by up to 4 fold [8]. A similar strategy was also used for α -santalene production with co-overexpression of a gene encoding alcohol dehydrogenase (*ADH2*), which converts ethanol to acetaldehyde [9]. Combination with over-expression of pathways draining cytosolic acetyl-CoA towards the product resulted in additional production increases [8, 9]. Furthermore, when the pathways competing for cytosolic acetyl-CoA were blocked by deleting the peroxisomal citrate synthase gene *CIT2* or/and cytosolic malate synthase gene *MLS1*, even higher production of α -santalene was achieved [9, 10]. These strategies have also been successfully applied in the production of 1-butanol [11], poly-(R)-3- hydroxybutyrate (PHB) [12], and biodiesel [13].

Besides the engineering strategies of the native pathways to increase cytosolic acetyl-CoA supply, several other strategies have been applied for different pathways for production of 1-butanol, biodiesel and PHB, such as the fungal phosphoketolase pathway [14, 15], bacterial pyruvate formate lyase pathway [16], ATP-citrate lyase pathway [17] and a bacterial PDH pathway [18].

1.1 Acetyl-CoA metabolism in yeast

Acetyl-CoA serves as a crucial intermediate metabolite in the metabolic network of *S. cerevisiae*, and its metabolism is highly compartmentalized as this metabolite is produced and used in the cytosol, mitochondria, peroxisomes and the nucleus (**Figure 1**). Acetyl-CoA is a key precursor metabolite for the synthesis of important cellular constituents such as fatty acids, sterols, and amino acids as well as the donor of acetyl unit for protein acetylation [19]. Besides these important functions it is also a precursor for many other biomolecules, such as polyketides, isoprenoids, 1-butanol and polyhydroxyalkanoids, which encompass many industrially relevant chemicals.

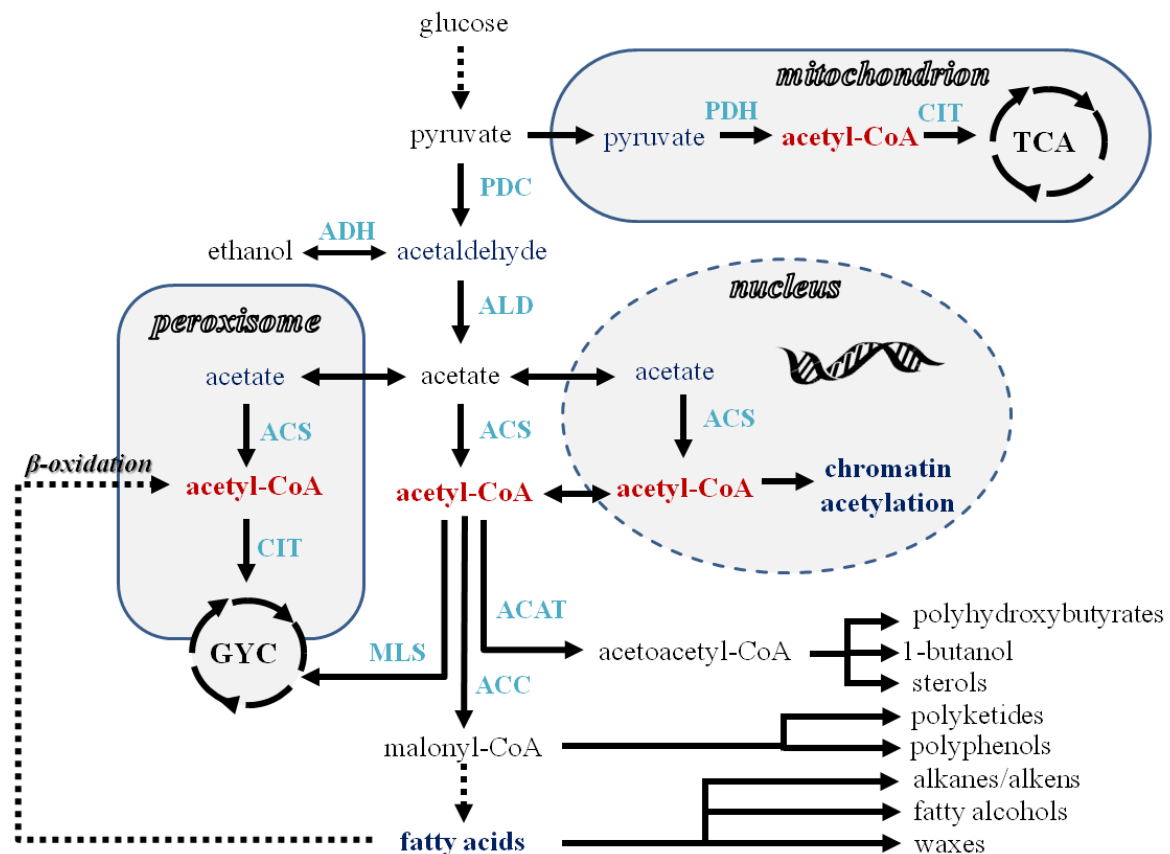


Figure 1. Overview of acetyl-CoA metabolism in yeast (Adapted from [6]).

1.1.1 Acetyl-CoA use in the TCA cycle and glyoxylate cycle

Acetyl-CoA is the key substrate for the TCA cycle, which plays a very important role in catabolism under glucose limited aerobic conditions. Acetyl-CoA used in the TCA cycle is generated by the pyruvate dehydrogenase complex (PDHC) from pyruvate, which is synthesized either in the cytosol via glycolysis from sugars, or from malate via malic enzyme located in the mitochondria. Acetyl-CoA is incorporated into the TCA cycle in a

step catalyzed by citrate synthase (CS), existing in two mitochondrial isoforms Cit1 [20] and Cit3 [21]. Citrate synthase (CS) condenses acetyl-CoA with oxaloacetate, yielding citrate, which is the first and generally considered to be the flux controlling reaction of the TCA cycle. Similarly to the TCA cycle, the glyoxylate cycle also begins with the condensation of acetyl-CoA and oxaloacetate, catalyzed by a peroxisomal CS isoform, Cit2. Another reaction involving acetyl-CoA in the glyoxylate cycle is catalyzed by malate synthase (MLS) encoded by *MLS1* [22], in which acetyl-CoA condenses with glyoxylate to form malate. The peroxisomal acetyl-CoA is formed directly from acetate by acetyl-CoA synthase.

PDHC is one of the largest and most complicated protein complexes known so far, and in yeast it consists of three main catalytic components termed and a fourth component. The three components are pyruvate dehydrogenase (encoded by *PDA1* and *PDB1*), dihydrolipoamide acetyltransferase (encoded by *LAT1*), dihydrolipoamide dehydrogenase (encoded by *LPD1*). The fourth component is called protein X (encoded by *PDX1*), and it is responsible to bind and position dihydrolipoamide dehydrogenase to dihydrolipoamide acetyltransferase [23-25]. In the irreversible reaction catalyzed by the PDH complex, pyruvate is converted to acetyl-CoA, CO₂ and NADH, with the participation of five cofactors (thiamin pyrophosphate, lipoic acid, flavin adenine dinucleotide, coenzyme A and NAD⁺). The PDH complex is regulated both at the transcriptional level, via the expression of its subunit gene *LPD1*, and post-transcriptional level, via the phosphorylation and dephosphorylation of its subunit Pda1 by a concerted activity of two kinases and two phosphatases [26-28].

CS has three isoforms in *S. cerevisiae*, encoded by *CIT1*, *CIT2*, *CIT3*. *CIT1* encodes the major functional isoform with an N-terminal mitochondrial targeting sequence [29-31]. *CIT2* encodes a peroxisomal isoform [32], with 81% identity with *CIT1* at the protein level and 74% identity at the DNA level. Its C-terminal signaling tripeptide SKL was found to be necessary and sufficient for directing Cit2 to the peroxisomes, which was called as the peroxisomal targeting sequence (PTS). However, the truncated Cit2 without the PTS resulted in a mislocalized form in the mitochondria, suggesting the presence of an additional signal sequence related with mitochondrial targeting [29], which was identified at its N-terminus in a later study [30]. *CIT3* encodes a minor functional isoform with an N-terminal mitochondrial targeting sequence as well [21], with 48% and 59% identity with *CIT1* at the protein level and DNA level, respectively, and with 47% and 61% identity with *CIT2*, respectively. Cit3 functions not only as a mitochondrial citrate synthase, but also as a methylcitrate synthase, which condenses propionyl-CoA and oxaloacetate to form 2-methylcitrate [33].

CIT1 expression is regulated by carbon sources, and repressed by glucose and further repressed by glucose and glutamate [34]. Like other TCA enzymes and those of electron

transport chain, its derepression was found to be regulated by the heme activator protein (HAP) system [35]. In the *CIT1* upstream sequence, three regulatory elements have been identified, one responsible for glucose repression, one for derepression [36], and an R box element [37] first identified as a binding site for the retrograde (RTG) transcription complex Rtg1-Rtg3 [38]. With detailed analysis of *CIT1* expression on different carbon sources, it was found that *CIT1* expression is dependent on *HAP* genes in cells with robust mitochondrial function, whereas its expression is dependent on *RTG* genes in cells with compromised mitochondrial respiratory capacity. Thus it was proposed that these different patterns were due to the requirement of sufficient glutamate for cell growth with reduced respiratory capacity [37].

CIT2 expression is also regulated by carbon sources, like *CIT1* expression [34]. In the *CIT2* upstream sequence, two R box elements were identified as the binding sites of the Rtg1-Rtg3 complex [38, 39], as mentioned above in the *CIT1* upstream sequence, which appears to be activated in a Rtg2-dependant fashion [40]. It was suggested that *CIT2* expression might be regulated by communication between the mitochondria and the nucleus, since its elevated transcription was observed in cells with dysfunctional mitochondria [41].

Disruption of *CIT1* results in several changes in the TCA cycle, such as its metabolite levels, decreases in enzyme levels and activities, reduced mitochondrial respiration of citrate and isocitrate, and inability to grow on acetate [42, 43]. The growth ability of a *cit1* Δ mutant on acetate could be restored by expressing the native Cit1, an inactive but a structurally unchanged Cit1 mutant [42], a mislocalized mitochondrial form of Cit2 [44], or additional Cit3 [21], but not by the cytosolic form of Cit1 [44]. One hypothesis for the growth inability on acetate was the dysfunction of the TCA cycle. It was also proposed that Cit1 with the normal conformation (even at an inactive state) is required for the formation of a TCA cycle enzyme complex in order to maintain α -ketoglutarate dehydrogenase complex activity.

MLS has two functional isoforms identified in *S. cerevisiae*, encoded by *MLS1* [22] and *DAL7* (or *MLS2*) [45], and Mls1 turned out to be the one responsible for the reaction in the glyoxylate cycle. Both proteins have the tripeptide targeting sequence SKL at their C termini, therefore it was predicted that they were localized in the peroxisomes. However, Mls1 seems to have dual localizations in the cytosol and peroxisomes. The two different localizations of Mls1 were first noticed when yeast was grown on ethanol or oleic acid, respectively [46], and later different distributions between the cytosol and the peroxisomes were also observed in different yeast mutants [10], indicating the possible presence of some regulatory mechanisms for its subcellular distribution which are still unclear.

MLS1 expression is also regulated by the carbon sources, the common response for genes involved in non-fermentative metabolism. In *MLS1* upstream sequence, two sites were identified as upstream activating sites (UASs), which could explain the transcriptional regulation of *MLS1* [47]. Both UASs turned out to be functional Carbon Source Responsive Elements (CSREs), which were found to be responsible for the transcriptional regulation of genes involved in acetyl-CoA generation and consumption (in the glyoxylate cycle and the subsequent gluconeogenesis), *ACS1* [48], *ICL1* [49], *MLS1* [47], *FBP1* [50] and *PCK1* [51].

1.1.2 Acetyl-CoA use in the PDH bypass

The PDH bypass is another important part in the metabolism of acetyl-CoA, especially cytosolic acetyl-CoA, consisting of pyruvate decarboxylase (PDC), acetaldehyde dehydrogenase (ALD) and acetyl-CoA synthetase (ACS). PDC converts pyruvate to acetaldehyde, and then acetaldehyde is converted to acetate by ALD, followed by the reaction catalyzed by ACS. The direct reaction for cytosolic acetyl-CoA biosynthesis is catalyzed by ACS. Two ACS isoforms were identified in yeast, encoded by *ACS1* and *ACS2*. These two isoforms differ from each other in a number of ways, *e.g.* enzymatic properties, subcellular localizations and immunological properties, and they were first recognized as ‘aerobic’ ACS and ‘anaerobic’ ACS, respectively [52-54].

The ‘aerobic’ and ‘anaerobic’ isoform were identified to be encoded by *ACS1* and *ACS2* [55], respectively. Although the tripeptide VKL at the C terminus of *Acs1* suggested its possible location in the peroxisomes, the experimental data about its subcellular localization seems quite complex and unclear, either in the mitochondria [56], peroxisomes [10], cytoplasm or nucleus [57]. *Acs1p* could be dually distributed in the cytosol and the peroxisomes based on its known functions [10], *e.g.* C₂ carbon source (ethanol or acetate) assimilation related with the glyoxylate cycle, lipid biosynthesis. The *Acs2* is 73.6% similar and 57.0% identical to *Acs1*. *Acs2* was identified as the ‘anaerobic’ isoform, since ACS activity seemed to be derived exclusively from *ACS2* in anaerobic, glucose limited chemostat cultures [58]. However, it was not appropriate to call *Acs2* as ‘anaerobic’ ACS, since *ACS2* is not only expressed under anaerobic conditions but also in aerobic conditions [58]. *Acs2* is thought to be localized in the cytosol due to no obvious targeting sequences at its terminus, which was also supported by a recent study [19].

Earlier enzyme assays and northern hybridization results revealed that *ACS1* expression was regulated by carbon sources, *i.e.* repressed by glucose and induced by C₂ carbon [59, 60]. In the *ACS1* upstream sequence, several transcriptional regulatory elements were identified, *i.e.* a CSRE, a binding site for the transcriptional factor *Adr1*, two distinct upstream repression sites (URS) and three binding sites for the pleiotropic factor *Abf1* [48, 60]. Under derepressed conditions, the CSRE and *Adr1* binding site were responsible

for the *ACS1* activation, which contributed to 45% and 35%, respectively. The activating function of Adr1 on *ACS1* transcription was further confirmed by its over-expression under both repressed and derepressed conditions. The negative function of the two URS1 was not affected under repressed or derepressed conditions. However, when a URS1-binding transcriptional factor encoding gene *UME6* was disrupted, significant *ACS1* expression was observed under repressed and derepressed conditions, and at least one functional Abf1 binding site was required for activated expression of *ACS1* under repressed conditions, but not under derepressed conditions. Therefore, it was proposed that Abf1 activates *ACS1* expression under repressed conditions, and that there could be a functional balance between the pleiotropic factor Abf1 and the general repressor Ume6. However under derepressed conditions, the positive control of two UAS elements (the CSRE and the Adr1 binding site) overruled the negative control of Ume6, and the activation of Abf1 was negligible.

ACS2 was considered to be constitutively expressed, since it was expressed in both aerobic and anaerobic conditions, and under aerobic conditions its expression did not show substantial differences on fermentable carbon sources (glucose) and non-fermentable carbon sources (ethanol) [58, 61]. In the upstream sequence of *ACS2*, a significantly similar region to the inositol/cholin-responsive element (ICRE) and three putative Abf1 binding sites were identified [61]. ICREs was previously identified as UASs of structural genes for membrane lipid biosynthesis, *e.g.* *FAS1*, *FAS2*, *INO1* [62], which interact with transcriptional factors, Ino2p/Ino4p (positive regulator) and Opi1p (negative regulator). The derepressed regulation of the ICRE obtained from *ACS2* was confirmed when it was inserted upstream of the reporter gene *lacZ*, and the activated expression caused by the ICRE was completely abolished in an *ino2Δ* null mutant, but no response in an *opi1Δ* null mutant. Abf1 binding sites were found in the upstream sequence of *ACS1* as well, and could contribute to the constitutive expression of *ACS2*, since Abf1 is required for the transcriptional activation of several house-keeping genes.

Although *Acs1* and *Acs2* belongs to the AMP-forming ACS family, which is usually post-transcriptionally regulated by acetylation of lysine in a conserved region [63-65], their acetylated regulation has not been identified yet. Amino acid alignments indicated that the reversible acetylation site is Lys675 in *Acs1*, and Lys637 in *Acs2*, respectively. In *Salmonella enterica*, when the lysine residue is acetylated in ACS, the adenylating activity of ACS is blocked in the first step, but the thioester-forming activity is not affected in the second step, and the deacetylation of inactive ACS is catalyzed by the NAD⁺-dependent protein deacetylase Sir2.

The *ACS1* disruption resulted in a prolonged lag phase in batch cultures with glucose [10, 55, 58], which might be explained by the 20-fold lower affinity of *Acs2* for acetate compared with that of *Acs1*, or the possible involvement of *Acs1* in chromatin regulation

[19]. However, these *acs1*Δ mutants were reported to behave quite differently in acetate or ethanol media. The *ACS2* disruption did not affect growth on acetate or ethanol, but resulted in growth inability on glucose due to the *ACS1* repression by glucose, since the *acs2*Δ mutant could grow in glucose limited chemostat cultures [10, 55, 58]. The double deletion *acs1 asc2*Δ mutant is not viable, which indicated that ACSs are indispensable for the survival of yeast cells.

1.1.3 Acetyl-CoA use in fatty acid and sterol metabolism

Acetyl-CoA is converted to malonyl-CoA by acetyl-CoA carboxylase (ACC) in the first and rate limiting step in fatty acid biosynthesis. During fatty acid degradation acetyl-CoA is generated via beta-oxidation in the peroxisomes, and is then consumed by the glyoxylate cycle as described above [66].

Two ACCs have been identified in *S. cerevisiae*, encoded by *ACCI* (or *FAS3*) and *HFA1*, which are localized in the cytosol and mitochondria, respectively [67, 68]. The localization of the two ACC isoforms indicates that they are responsible for fatty acid biosynthesis in different subcellular compartments. The *ACCI* expression is regulated by transcriptional factors, *e.g.* Ino2, Ino4, Opi1, which are also responsible for the regulation of phospholipid metabolism [69], as reviewed in [70]. *In vitro* studies revealed that Acc1 can be rapidly phosphorylated and inactivated by mammalian carboxylase kinases, *e.g.* AMP-activated protein kinase (AMPK) [71, 72]. One phosphorylation site at Ser1157 first identified by phosphoproteome analysis and another putative site at Ser659 have been suggested to be the targets of Snf1, a member of AMPK family in yeast [73]. A recent study has revealed that Acc1 is under the post transcriptional regulation of Snf1, in order to maintain an appropriate distribution of acyl-chains of different length [74].

In sterol biosynthesis, two acetyl-CoA molecules are condensed into one acetoacetyl-CoA molecule in the first step. The reaction is catalyzed by acetoacetyl-CoA thiolase (ACAT), encoded by *ERG10* in *S. cerevisiae* [75].

1.1.4 Acetyl-CoA transport between subcellular organelles

Acetyl-CoA metabolism is highly compartmentalized in *S. cerevisiae*, as well as in other fungi, and it cannot travel freely between different subcellular organelles [76]. Three transport systems have been proposed for the acetyl-CoA transportation between these organelles in fungi, *i.e.* the carnitine/acetyl-carnitine shuttle, C₄ dicarboxylic acid synthesis from acetyl-CoA via the glyoxylate cycle (as discussed above), and acetyl-CoA re-generation from citrate by ATP citrate lyase (ACL) in the cytosol [77]. Two of them have been identified in *S. cerevisiae* except ACL [78].

Carnitine cannot be synthesized *de novo* in *S. cerevisiae* [79], but extracellular carnitine can be transported into the cells by a plasma membrane transport protein Hnm1 [80, 81]. In *S. cerevisiae*, besides the carnitine transporter Hnm1, four other enzymes have been identified to be involved in the carnitine/acetyl-carnitine shuttle, encoded by *YAT1*, *YAT2*, *CAT2*, *CRC1*, respectively. *YAT1*, *YAT2* and *CAT2* encode carnitine acetyltransferases (CATs), which catalyze the reversible reactions of acetyl group transfer between coenzyme A and carnitine. The intermediate acetyl-carnitine can cross the membranes of the mitochondria or the peroxisomes as the transportable molecule. Mitochondrial and peroxisomal Cat2 has been identified as the main CAT [82], Yat1 as a second one associated with the outer mitochondrial membrane [83], and Yat2 as a third one which mostly contributes when cells are grown on ethanol [84]. Crc1 is identified as a carnitine acetyl-carnitine translocase in the inner mitochondrial membrane [85].

1.1.5 Acetyl-CoA in protein acetylation

Besides serving as a crucial node in the network of carbon metabolism, acetyl-CoA plays an important part in regulatory network, *i.e.* protein acetylation as acetyl donor. Protein acetylation at α - or ϵ -amino groups during post-translational modification processes has been found to be important for regulation in both eukaryotes and prokaryotes [86, 87]. Histone acetylation affects chromatin structure and regulates gene transcription via different interactions [88]. Non-histone protein acetylation modulates cellular signaling at multiple levels, *e.g.* mRNA stability, protein localization, protein interaction, protein degradation or protein function [89, 90]. A number of histone acetyltransferases (HATs) and histone deacetylases (HDACs) have been identified in *S. cerevisiae*, which are responsible for the acetylation and de-acetylation of histone and non-histone proteins, but for most of them, their functions as transcriptional regulators are still under investigation [91].

It has been suggested that the nucleocytoplasmic acetyl-CoA abundance directly regulates the dynamic acetylation and deacetylation of proteins. Acs2 and Acs1 are required for histone acetylation as one major source and a secondary source of acetyl-CoA [19]. Decreased activity of Acc1, which consumes acetyl-CoA for *de novo* synthesis of fatty acids, resulted in increased histone acetylation and altered transcriptional regulation [92]. Using a continuous culture system termed the yeast metabolic cycle (YMC), Tu *et al.* found that acetyl-CoA drives the transcriptional growth program by promoting the acetylation of histones at growth related genes in yeast [93, 94], and they predicted that ‘intracellular acetyl-CoA fluctuations might represent a distinctive gauge of cellular metabolic state that could be decoded by way of dynamic acetylation and deacetylation reactions’ [95].

1.2 Non-ethanol producing strains for biochemical production

When yeast is grown on glucose under aerobic conditions, the majority of the glycolytic flux is directed towards ethanol due to the so-called Crabtree effect. Ethanol is usually the main by-product when yeast serves as a cell factory for biochemical production. In order to efficiently convert glucose to the desired products, a non-ethanol producing yeast strain would be an interesting platform for the production of biochemicals. An obvious strategy to eliminate ethanol production is to simply remove alcohol dehydrogenase (ADH) activity to prevent conversion of acetaldehyde to ethanol. However, yeast contains a very large number of ADH enzymes besides the major isoform Adh1 [96], and many of the specific product pathways may also rely on ADH activity, e.g. 1-butanol biosynthesis. It is therefore inherently difficult to eliminate ethanol production in yeast. The only strategy that has worked so far is removing pyruvate decarboxylase (PDC) activity through deletion of all three genes that encode this activity.

1.2.1 Pyruvate decarboxylase

Pyruvate decarboxylase converts pyruvate, the end product of glycolysis to CO₂ and acetaldehyde, the direct precursor of ethanol. In *S. cerevisiae*, PDC is encoded by three structural genes, *PDC1*, *PDC5* and *PDC6* [97-99]. Pdc1 is the major PDC isoform, while Pdc5 and Pdc6 are two minor isoforms.

PDC1 was cloned and identified from isolated mutants with no or reduced PDC activities [100]. *PDC1* is strongly expressed in actively fermenting yeast cells. Disruption of *PDC1* resulted in decreased activity, suggesting the presence of a second PDC gene [97], which was later identified as *PDC5* [98, 101]. Pdc5 is found to be 88% identical with Pdc1, and also function during glycolytic fermentation. However, *PDC5* is expressed only in the absence of *PDC1* or under thiamine limitation [102]. Both *PDC1* and *PDC5* are under *PDC* auto-regulation, which means they could substitute each other. The auto-regulation has been observed for other genes, e.g. histone encoding genes. Pdc6 was identified using low-stringency Southern blot analysis [99]. *PDC6* expression is induced by nonfermentable carbon sources (ethanol) and also dramatically induced under conditions of sulfur limitation. Disruption of *PDC6* did not change the phenotype or the enzyme activity, as well as disruption of *PDC6* in a *pdc1*Δ mutant or a *pdc5*Δ mutant.

Disruption of both *PDC1* and *PDC5* resulted in undetectable PDC activity and impaired growth in complex medium with glucose [98]. However, deletion of only *PDC1* and *PDC5* can lead to mutants with increased *PDC6* expression, in which *PDC6* was spontaneously fused under *PDC1* promoter via recombination [103]. Thus, triple deletion is necessary for a non-ethanol producing yeast strain.

1.2.2 Pyruvate decarboxylase negative strain

Although *pdc* triple deletion mutants (*pdc1* Δ *pdc5* Δ *pdc6* Δ , also called Pdc negative strains) have the potential to be non-ethanol producing platform for biochemical production, they cannot grow on glucose as the sole carbon source [104].

When C₂ carbon was supplemented, the Pdc negative strain could grow in glucose-limited chemostat cultures using minimal medium, but not in batch cultures. When glucose was fed instead of the glucose-C₂ carbon mixture or C₂ carbon into the chemostat cultures, the cells of the Pdc negative strain were washed out [104]. With excess glucose pulsed into the steady chemostat cultures, a small increase in glycolytic flux was observed in the Pdc negative strain as well as pyruvate excretion, which was not caused by a decreased flux from pyruvate to the TCA cycle, since PDH activity did not show a strong decrease after a glucose pulse [105]. The growth requirements of C₂ carbon supplementation indicated that the growth defect of Pdc negative strain on glucose was due to the lack of cytosolic acetyl-CoA for biosynthesis of cellular biomolecules, especially lipids [78]. However, addition of carnitine does not restore growth of a Pdc negative strain in chemostat cultures using glucose as sole carbon source. In addition, by over-expressing threonine aldolase (encoded by *GLY1*), the growth of the Pdc negative strain on glucose could be restored, since that Gly1 releases acetaldehyde from threonine, which can be converted to acetyl-CoA via acetate in the cytosol.

Interestingly, the Pdc negative strains are sensitive to high glucose even when supplemented with a C₂ carbon source or with *GLY1* over-expression [78, 106]. van Maris *et al.* performed directed evolution of a Pdc negative strain on glucose [107]. During the evolution, the Pdc negative strain RWB837 was evolved in a glucose-limited chemostat culture supplemented with gradually reduced ethanol for five consecutive steps, yielding the C₂-independent Pdc negative strain RWB837*. Subsequently, RWB837* was evolved in shake flasks using minimal medium with gradually increased glucose by serial transfer, yielding the ‘C₂-independent, glucose-tolerant, and pyruvate-hyperproducing’ strain TAM. The TAM strain could grow on glucose as the sole carbon source, with a maximum specific growth rate of 0.20 h⁻¹ in minimal medium with 10% glucose. The transcriptome analysis revealed a number of changes in TAM compared to the wild type strain CEN.PK 113-7D, *e.g.* over-representation of Mig1 regulated genes, down-regulation of *HXT* genes, up-regulation of *GLY1* (but still low enzyme activity). The pyruvate-hyperproducing capacity of TAM makes it an important platform strain for industrial production of pyruvate or pyruvate-derived chemicals, without producing ethanol.

In a later study, an *MTH1* allele with a 225 bp internal deletion (*MTH1-ΔT*) was identified in the TAM strain, and was found to be responsible for growth recovery of the Pdc negative strain on glucose [108].

Mth1 functions as a negative transcriptional regulator in the glucose signaling pathway together with other regulators, *i.e.* Snf3, Rgt2, Std1, Rgt1. Mth1 or its paralog Std1 interacts with Rgt1, which also interacts with other transcription factors, *e.g.* Cyc8, Tup1, and binds the promoters of hexose transporter genes [109, 110]. Besides the *MTH1-ΔT* allele, several other *MTH1* alleles have been identified in selections of glucose or catabolite repression suppressors using other glucose sensitive mutants [111-115]. The *MTH1* alleles seemed to be able to resolve the glucose sensitive problem in these mutants. Previous studies have shown that these *MTH1* alleles reduced glucose transport by repressing the transcription of several hexose transporter genes (*HXTs*) [107, 111, 113, 114], as well as over-expression of *MTH1* [108]. It has been proposed that *MTH1-ΔT* resulted in a decreased degradation of Mth1 [108], which could be related to putative PEST sequences (usually present in proteins with short intracellular half-life) and a target site for phosphorylation by casein kinase Yck1 [116], which are situated inside the deleted region. The decreased degradation of Mth1 resulting from the *MTH1-ΔT* allele, could prevent the phosphorylation of Rgt1, which was required for its release from the promoters of several hexose transporters [110], and therefore repress the transcription of hexose transporter genes even during growth on high glucose.

However, when introducing the *MTH1-ΔT* allele into an un-evolved Pdc negative strain, the growth rate ($\mu_{\max}=0.10 \text{ h}^{-1}$) was slower in minimal medium with 2% glucose, compared to the TAM strain ($\mu_{\max}=0.20 \text{ h}^{-1}$), indicating the possible presence of additional advantageous genetic changes in the TAM strain besides *MTH1-ΔT*.

1.3 Metabolic engineering and adaptive evolution in strain development

Traditionally in industry, microorganisms that naturally produce a desired molecule were identified and then improved through classical strain engineering based on mutagenesis and screening. This has been an efficient approach and has resulted in low-cost production processes for many different chemicals, *e.g.* penicillin, citric acid and lysine . This approach is usually referred to as adaptive laboratory evolution (referred to as adaptive evolution in this thesis except when otherwise specified), experimental engineering, or evolutionary engineering [117]. However, this type of strain development typically leads to a slow, incremental increase in strain performance, especially in the later stages of strain improvement. Moreover, the unknown mechanisms underlying strain improvement precludes the rapid transfer of relevant traits among different strains or species.

With the introduction of genetic engineering and methods for detailed analysis of cellular metabolism it became possible to use a more directed approach to improve cell factories, generally referred to as metabolic engineering [118]. Today metabolic engineering has evolved into a research field that encompasses detailed metabolic analysis with the objective to identify targets for metabolic engineering and the implementation of metabolic engineering strategies for improvement and/or design of novel cell factories [119]. With help from synthetic biology, another research field that originally aimed at reconstruction of small, artificial biological systems (*e.g.* assembling a new biological regulon or oscillators for gene expression regulation in response to a specific input), metabolic engineering offers tremendous opportunities to create novel cell factories that are tailor made for efficient production of fuels and chemicals [120-122]. However, this rational strategy is not always perfect since it is based on existing knowledge. Especially in the case of synthetic pathway introduction, when designing and building non-native pathways, it needs to be optimized for strain fitness and biochemical production, which is not only related to the metabolic fluxes but also associated with regulation systems, which is always complicated and not well characterized yet.

Recently, with impressive progresses achieved in systems biology and bioinformatics, rapid, affordable, high throughput techniques for genome, transcriptome, proteome, and metabolome analysis become accessible for adaptively evolution, and whole genome sequencing is found to be superior to other analytical techniques, since the genetic changes can be immediately and exactly reconstructed in native strains [123]. Therefore it is possible to link the phenotypes with the genotypes. Using ‘reverse’ metabolic engineering, or ‘inverse’ metabolic engineering, the genetic changes responsible for the changes in phenotypes can be identified [124-127], which will elucidate underlying mechanisms for improved performance of adaptively evolved strains. As reviewed in

[117], through microbial adaptive evolution, interactions between these mutations identified by genome sequencing are very common, and adaptive mutations frequently target regulatory mechanisms. And it is pointed out that ‘principles of systems-level optimization underlie the genetic changes seen in adaptive evolution, and with a systems-level understanding, these optimization principles can be harnessed for the purposes of metabolic engineering’ [117].

Therefore, adaptive evolution harnesses the biology power for metabolic engineering [128], which could be finally applied in the development and performance improvement of cell factories

Chapter 2. Overview of the thesis

The objective of this study is to develop a non-ethanol producing platform strain of *S. cerevisiae* as a cell factory, which can convert glucose to cytosolic acetyl-CoA for biochemical production.

A Pdc negative strain has the potential to be a non-ethanol producing strain for biochemical production. However, it cannot grow on glucose as the sole carbon source and requires supplementation of acetate or ethanol to the medium in order to meet the requirement for acetyl-CoA in the cytosol (needed for biosynthesis of fatty acids and ergosterol). Therefore, such a strain cannot directly serve as a platform cell factory for acetyl-CoA derived products. This limitation was partially solved by evolving the Pdc negative strain, resulting in a glucose tolerant and C₂ independent mutant TAM [129]. Its mechanisms for growth recovery were identified to be related to an in-frame internal deletion in *MTH1*. The *MTH1-ΔT* allele resulted in reduced glucose uptake, which may attenuate the repression on respiratory metabolism. However, it is not addressed what mechanism could provide the cells with sufficient precursors for the synthesis of cytosolic acetyl-CoA. In addition, the Pdc negative strain with the *MTH1-ΔT* allele does not efficiently convert pyruvate to acetyl-CoA in the cytosol.

For the reasons above, all reactions related with acetyl-CoA and C₂ carbon were filtered from the latest Genome Scale Metabolic Model of *S. cerevisiae* [130] for the possible routes to supply cytosolic acetyl-CoA in Pdc negative strains. One route was identified to be the source of cytosolic acetyl-CoA in Pdc negative strains (Paper I). In addition, adaptive evolution of Pdc negative strains on glucose was performed using serial transfer, and genome sequencing results revealed several genetic changes in evolved strains (Paper II). With all the findings, possible mechanisms were proposed for growth recovery of evolved Pdc negative strains on glucose, which would be useful for the fundamental understanding of acetyl-CoA metabolism in yeast, as well as yeast strain development for biochemical production as cell factories. Finally, the pyruvate formate lyase pathway was introduced into the reverse engineered Pdc negative strain with the *MTH1-ΔT* allele, which further increased the cytosolic acetyl-CoA supply and therefore increased the final biomass.

PAPER I. Ach1 is involved in shuttling mitochondrial acetyl units for cytosolic C₂ provision in Pdc negative *Saccharomyces cerevisiae*

In yeast, acetyl-CoA is compartmentalized and not directly transported between these subcellular compartments. As described before, with the acetyl-carnitine or glyoxylate shuttle, acetyl-CoA produced in the peroxisome or the cytoplasm can be transported into the cytoplasm or the mitochondria. However, it is still unclear whether acetyl-CoA

generated in the mitochondria can be exported to the cytoplasm. Here we investigated this using a Pdc negative, non-fermentative strain, and aimed at identifying the mechanism responsible for the exchange of acetyl units between the mitochondrial matrix and the cytoplasm in *S. cerevisiae*. Our results identified a route relying on Ach1 that could transfer acetyl units from mitochondria to the cytoplasm. Based on our results we propose a new route in which acetyl units are shuttled from the mitochondria to the cytoplasm in the form of acetate.

PAPER II. Adaptive mutations in sugar metabolism restore growth on glucose in a pyruvate decarboxylase negative yeast strain

In this study, a collection of Pdc negative strains was constructed and one of them was adaptively evolved in glucose medium via serial transfer in three independent cell lines, yielding three independently evolved strains. The evolved Pdc negative strains can grow in minimal medium with glucose as the sole carbon source at maximum specific rates of 0.138 h^{-1} , 0.148 h^{-1} , 0.141 h^{-1} , respectively. Several genetic changes were identified in the evolved Pdc negative strains by genomic DNA sequencing, including 4 genes carrying point mutations in at least two of the evolved strains: a transcription factor gene of the glucose-sensing signal transduction pathway *MTH1*, a hexose transporter gene *HXT2*, a mitochondrial citrate synthase gene *CIT1*, and a histone deacetylase gene *RPD3*. Reverse engineering of the parental Pdc negative strain through introduction of the *MTH1*^{81D} allele restored its growth on glucose. The non-synonymous mutations in *HXT2* and *CIT1* may function in the presence of the mutations in *MTH1* and could be related to the cytosolic acetyl-CoA supply in Pdc negative strains.

Paper III. Functional pyruvate formate lyase pathway expressed with its cofactors in *Saccharomyces cerevisiae* at aerobic growth

In connection with establishing yeast platforms for production of fuels and chemicals it is necessary to engineer their metabolism such that the raw material can be efficiently converted to the product of interest. Many industrially interesting products are biosynthesized from acetyl-CoA [6] and there is therefore much interest in efficient conversion to acetyl-CoA. In yeast, acetyl-CoA metabolism is compartmentalized into three main compartments, the mitochondria, the cytosol and the peroxisome, and cytosolic acetyl-CoA is generally preferred for efficient production of heterologous products [6]. Naturally cytosolic acetyl-CoA is converted from acetaldehyde with ATP consumed, which translates to a yield loss in the overall conversion of glucose to the product of interest. There is therefore much interest in heterologous pathways which are more efficient than the endogenous pathway.

An alternative pathway is pyruvate formate lyase (PFL), and PFL is characterized as an enzyme functional at anaerobic conditions, since its active form is sensitive to oxygen. In this study, PFL gene and its activating enzyme gene from *E. coli* were expressed in a Pdc negative yeast with a mutation in the transcriptional regulator Mth1, IMI076 (Pdc⁻ *MTH1-ΔTura3-52*). Two different cofactors were co-expressed with the PFL pathway as electron donors, reduced ferredoxin or reduced flavodoxin, respectively, which were found to have positive effects on growth under aerobic conditions, i.e. a higher final biomass concentration and a significant increase in transcription of formate dehydrogenases (FDHs). Among the two cofactors reduced flavodoxin was found to be a better electron donor for the PFL pathway than reduced ferredoxin.

Chapter 3. Results and discussion

3.1 Ach1 compensates cytosolic acetyl-CoA in Pdc negative strain

As mentioned before, a Pdc negative strain cannot grow on glucose as the sole carbon source due to the lack of cytosolic acetyl-CoA, and the *MTH1-ΔT* allele could restore its growth on glucose which resulted in reduced glucose uptake. However, the source of cytosolic acetyl-CoA is still a mystery in a Pdc negative strain with *MTH1-ΔT* allele. Using the latest Genome Scale Metabolic Model of *S. cerevisiae* [130], 57 reactions were found related with C₂ compound metabolism, including 34 reactions directly related with acetyl-CoA metabolism and transport, and 23 more reactions involved in metabolism of other C₂ compounds such as ethanol, acetaldehyde and acetate.

Without carnitine supplemented, there could be two possible routes to provide cytosolic acetyl-CoA in a Pdc negative strain, after analyzing the possible roles of these 57 reactions in cytosolic acetyl-CoA supply. One possible route is catabolizing threonine via threonine aldolase (encoded by *GLY1*) to release acetaldehyde, which can be converted to acetyl-CoA via acetate in the cytosol. A previous study has revealed that *GLY1* over-expression in a Pdc negative strain can circumvent the essential biosynthetic role of pyruvate decarboxylase when cultured in glucose limited chemostat conditions [106]. However, the possibility of the route involving Gly1 for cytosolic acetyl-CoA supply was excluded due to its low affinity for threonine and the relatively low intracellular threonine concentration when yeast is grown on excess glucose [129].

The other potential route is converting acetyl-CoA to acetate in the mitochondria, followed by transport of acetate across the mitochondrial membranes to the cytosol, and conversion of acetate into acetyl-CoA by cytosolic acetyl-CoA synthetase (ACS). One gene product, encoded by *ACHI*, is associated with both acetyl-CoA and acetate in the mitochondria, although its functions are not conclusive yet. Ach1 was originally proposed as an acetyl-CoA hydrolase to catalyze the scission of acetyl-CoA into acetate and CoA [131-134], like many other acetyl-CoA hydrolases found in mammalian tissues [135, 136]. The exact catalytic role of this enzyme was questioned by the observations of its role in acetate but not ethanol utilization [133]. It was proposed that this enzyme may have a novel function concerning acetyl-CoA metabolism, but it was only recently that Fleck and Brock characterized Ach1 as a CoA transferase involved in mitochondrial acetate detoxification, not just wasting energy by hydrolyzing acetyl-CoA [137]. In their study Ach1 showed the highest specific activity for the CoA transfer from succinyl-CoA *in vitro*. However, the substrate promiscuity of this enzyme did not exclude its transferase activity on other CoAs. We therefore proposed that this enzyme can transfer CoA unit from acetyl-CoA to succinate, forming acetate and succinyl-CoA.

To test our assumptions, we first evaluated the effects of succinate supplementation in a Pdc negative strain IMI076 carrying *MTH1* with an internal deletion (*MTH1-ΔT*) [108] and a wild type strain CEN.PK113-5D [138]. The cultivations were performed in minimal medium with 2% glucose using Bioscreen C. When 0.5 g/L succinate was added to the medium, there was no obvious growth difference for the wild type, but it was clear that external succinate supplementation shortened the lag phase for IMI076 (**Figure 2A**). This was further confirmed by culturing IMI076 in shake flasks supplemented with 0.5 g/L succinate. As shown in **Figure 2B**, the lag phase was shortened by about 22 h. This result was consistent with increased rates of glucose consumption and pyruvate accumulation (data not shown).

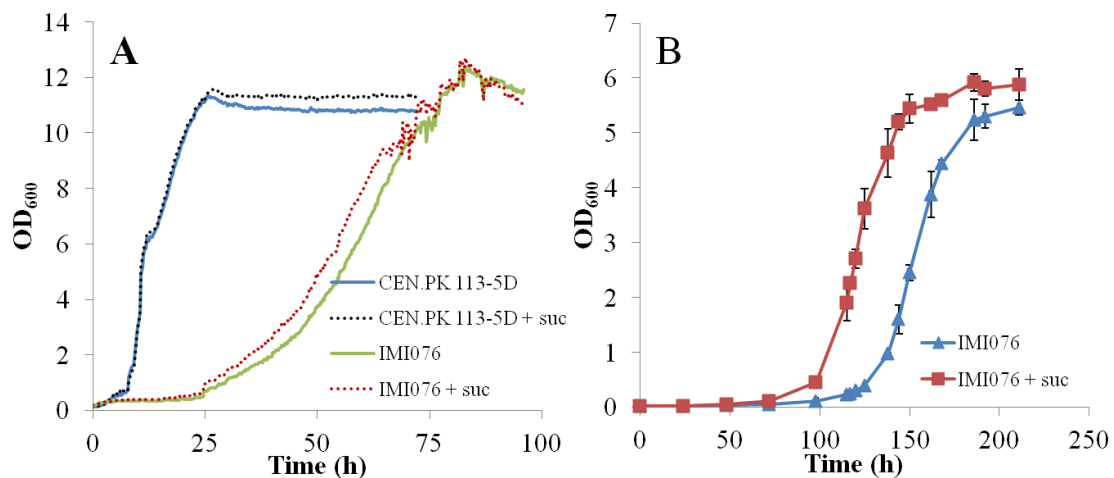


Figure 2. Addition of succinate improves the growth of the strain IMI076 (Pdc⁻ *MTH1-ΔT*) in minimal medium with glucose as the sole carbon source using Bioscreen (A) and shake flask (B).

To test if Ach1 is a key player in channeling acetyl units from the mitochondria to the cytosol, *ACH1* was replaced with a functional *URA3* cassette in IMI076, yielding YACH01. As control, IMI076 was transformed with an empty plasmid pSP-GM1 [139] containing the same *URA3* cassette, yielding YACH00.

As shown in **Figure 3A**, when cultured on synthetic dextrose (SD) plates supplemented with uracil (SD+ura), no big growth difference between IMI076 and YACH00 was observed, but significantly impaired growth of YACH01. When ethanol was supplemented, all strains with or without *ACH1* deletion grew well on glucose with no difference (**Figure 3A**). These results suggested that *ACH1* is important for its growth on glucose as the sole carbon source. The spot assay results of the Pdc negative strains could be affected by the SD+ura agar plate used, since it could contain threonine or other C₂ contaminations as speculated by Oud *et al.* [108]. To exclude any potential C₂ contamination in the medium, the strains were cultured in liquid minimal medium with glucose as the sole carbon source. Cells of IMI076 and YACH01 were harvested during

exponential phase and washed twice after pre-cultured in minimal ethanol media, and then inoculated to the minimal glucose media. IMI076 grew normally as described before [139], with a specific growth rate of about 0.07 h^{-1} , whereas YACH01 could not grow on glucose as the sole carbon source (**Figure 3B**).

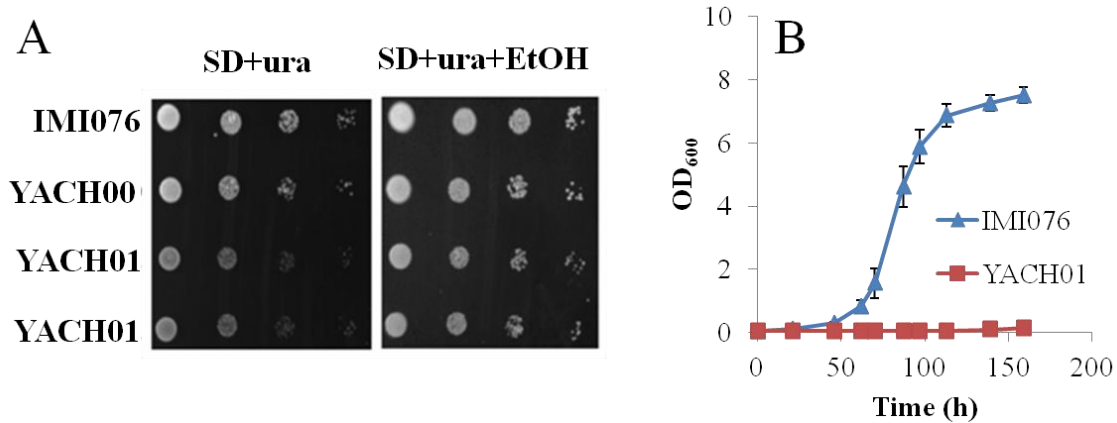


Figure 3. The growth of the strain IMI076 (*Pdc⁻ MTH1-ΔT*) relies on *Ach1*. A) Spot assays on synthetic media with glucose or glucose plus ethanol. The plates were incubated at 30 °C and recorded photographically 4 days after inoculation. B) Growth assays in liquid minimal media with glucose as the sole carbon source. Cells were precultured in minimal media with ethanol, and washed twice before inoculation into minimal glucose media. Data are mean +/- standard error of three biological replicates.

The inability of growth on glucose as the sole carbon source that resulted from *ACH1* disruption points to this enzyme being essential for the cytosolic acetyl-CoA supply, which might be transferred from the mitochondria. To further confirm this hypothesis we performed complementation of the *ach1* deletion strain with the wild-type gene and a truncated version of *ACH1* (*tACH1*), respectively. The truncated version of *Ach1* is mislocalized in the cytoplasm due to the absence of its N-terminus [134]. *ACH1* and *tACH1* were reintroduced into the *ach1* mutant YACH01 by chromosomal integration, yielding YACH02 and YACH03, respectively. Growth assays of the two resulting strains revealed that complementation with the intact *ACH1* gene could restore growth of the *ach1* mutant, but not the truncated *ACH1* (**Figure 4**). The maximum specific growth rate of the strain YACH02 was increased by 52% compared with the strain IMI076, which may be ascribed to increased *ACH1* expression in YACH02, in which *ACH1* was expressed under the strong constitutive promoter *TEF1*.

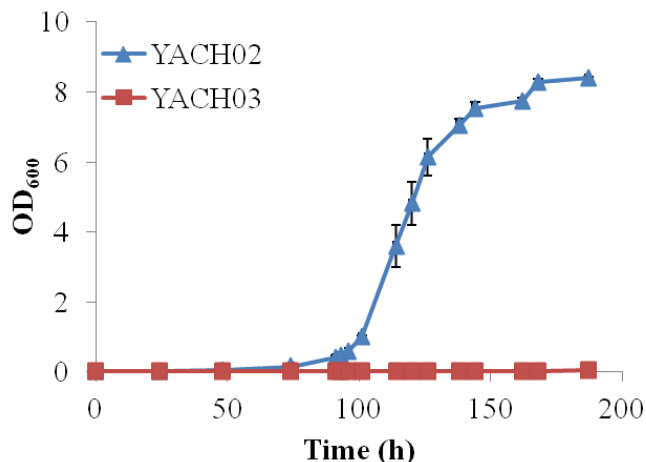


Figure 4. Complementation with the intact *ACH1* but not the truncated version restores growth of an *ach1* mutant. Cells were precultured in defined minimal media with ethanol, and then washed twice with sterile water before inoculation into glucose media. All measurements are mean +/- standard error of three biological replicates.

To further validate the hypothesis that the cytosolic acetyl-CoA in IMI076 is likely to come from mitochondrial acetyl-CoA, we therefore cultivated it in absence or presence of UK-5099. The compound UK-5099, an analogue of alpha-cyanocinnamate is a specific and potent inhibitor of the mitochondrial pyruvate carrier [140, 141]. In yeast, the pyruvate uptake into the mitochondria is reduced by more than about 70% with 0.2 mM UK-5099 supplemented, compared to that without inhibitor in yeast [141]. Mitochondrial acetyl-CoA is exclusively converted from pyruvate, catalyzed by the pyruvate dehydrogenase complex. Therefore in the presence of UK-5099, inhibiting mitochondrial pyruvate uptake will limit the availability of acetyl units in this compartment, which will further restrict the supply of cytosolic acetyl-CoA and therefore affect the growth of cells.

As shown in **Figure 5A**, when 0.2 mM UK-5099 dissolved in DMSO was added to the culture during the exponential growth phase, a significant decrease in growth was observed, compared with the control experiment with same amount DMSO but no inhibitor added. Furthermore, there was no significant effect on the growth of the wild type strain CEN.PK 113-5D when supplemented with 0.2 mM UK-5099 (**Figure 5B**). The maximum specific growth rate of the strain IMI076 showed a big decrease upon the addition of UK-5099, from 0.066 h^{-1} to 0.018 h^{-1} . These observations clearly shows that the flux of mitochondrial pyruvate uptake is limiting the growth of the Pdc negative strain, which again supports the hypothesis that cytosolic acetyl-CoA is derived from mitochondrial acetyl-CoA, which is related to Ach1.

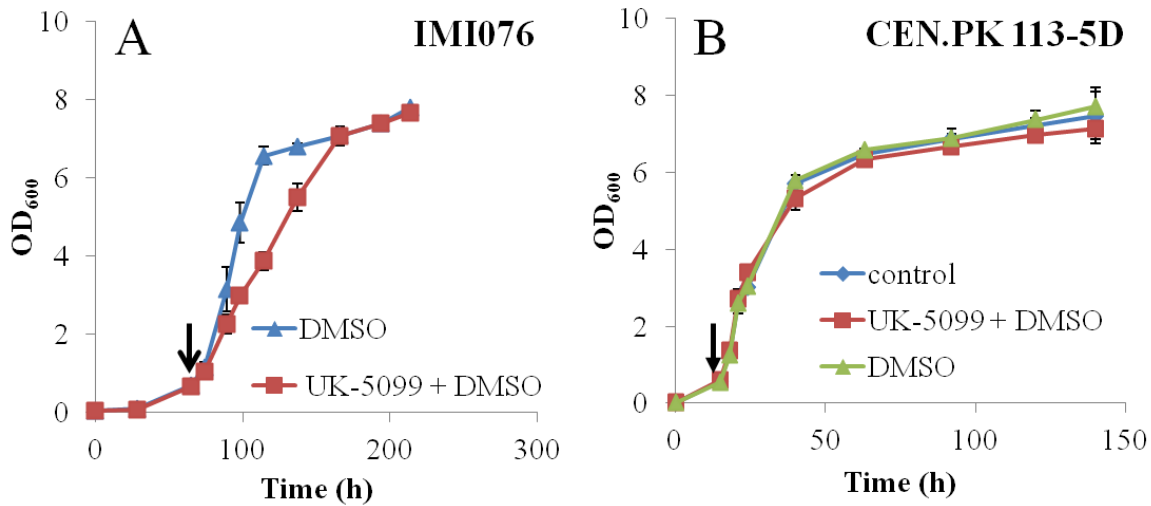


Figure 5. Growth assays of IMI076 (A) and CEN.PK 113-5D (B) upon addition of UK-5099 in minimal medium with glucose as the sole carbon source. Arrows represent the addition of UK-5099 dissolved in DMSO or DMSO without UK-5099. All measurements are mean +/- standard error of three biological replicates.

To summarize, inspired by the function as a CoA transferase and the promiscuity of this enzyme on its substrates, we hypothesized that Ach1 could transfer CoA from acetyl-CoA to succinate. The succinate supplementation results showed that addition of succinate improves growth of the strain IMI076, but has no impact on the growth of the wild type strain (**Figure 2**). When *ACH1* was disrupted in IMI076, the growth on glucose was interrupted (**Figure 3**), clearly indicating that Ach1 plays an important role in the growth of the Pdc negative strain on glucose. Moreover, the complementation of the *ACH1* gene under control of the strong *TEF1* promoter, not only rescued the growth on glucose but resulted in slightly faster growth than the IMI076 strain (**Figure 4**), further confirming that Ach1 is involved in cytosolic acetyl-CoA supply. It is also found that a truncated version of Ach1 localized in the cytosol could not rescue growth of IMI076 with *ach1* deletion, and that inhibition of the mitochondrial pyruvate carrier reduces growth of IMI076, which further confirmed that the cytosolic acetyl-CoA comes from the mitochondria.

Based on these results we propose a new route for acetyl-CoA transfer in the Pdc negative strains. Here *S. cerevisiae* uses acetate instead of citrate to transfer acetyl units from the mitochondria to the cytosol. This alternative shuttle route has been reported in other eukaryotes, e.g. *Trypanosoma brucei* [142]. As shown in **Figure 6**, when cells grow on glucose, acetyl-CoA produced in the mitochondria can be converted to acetate potentially through the reversible CoA transferase Ach1. Acetate can cross the mitochondrial membrane and be converted into acetyl-CoA in the cytosol. It has been reported that Ach1 is repressed by glucose, since its expression level increased in late exponential phase compared to the early exponential phase [132]. In IMI076, the *MTH1*-

3.2 Growth recovery through adaptive evolution and reverse metabolic engineering

To construct Pdc negative strains, *PDC1*, *PDC5*, and *PDC6* were consecutively deleted using a bipartite strategy [143] as shown in **Figure 7**, in two different background strains, CEN.PK 113-5D (*MATa ura3-52*) and CEN.PK 110-10C (*MAT α his3- Δ 1*) [138]. Combined with strain crossings and tetrad segregations, a collection of triple deletion mutants was constructed carrying different auxotrophic markers: *ura3-52*, *his3- Δ 1* or *ura3-52 his3- Δ 1*, as shown in **Figure 8**, which will allow for synthetic gene introduction using up to two marker genes.

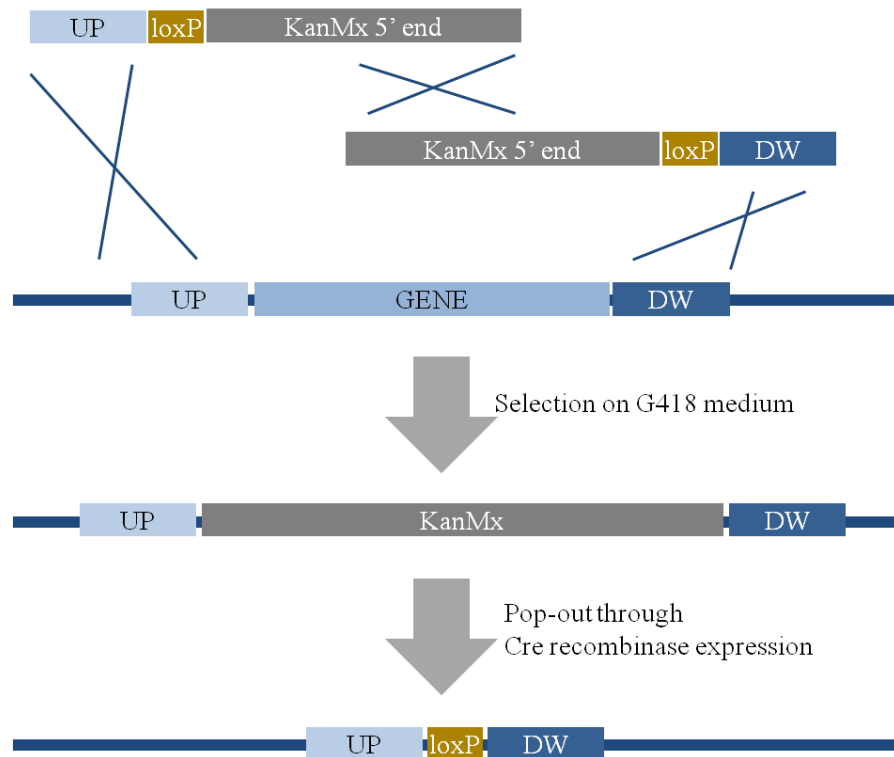


Figure 7. Bipartite strategy for gene deletion. Sequences upstream and downstream of the individual genes and two overlapping fragments of the *kanMX* resistance marker cassette flanked by *loxP* sites were PCR amplified. The two fused PCR fragments for each gene deletion were transformed into yeast using the lithium acetate method [144]. After each gene deletion, the *kanMX* marker cassette was looped out via Cre recombinase mediated recombination between the two flanking *loxP* sites using plasmid pUC47 or pUG62 as described previously [145].

In order to gain more insights into the possible evolving mechanisms of Pdc negative strains, adaptive evolution of a Pdc negative strain CEN.PK YMZ-E1 (*MATa ura3-52 his3- Δ 1 pdc1 Δ pdc5 Δ pdc6 Δ*), E1 for short, was performed in glucose medium via serial transfer. Afterwards, the genetic changes in the evolved Pdc negative strains were identified using genomic DNA sequencing.

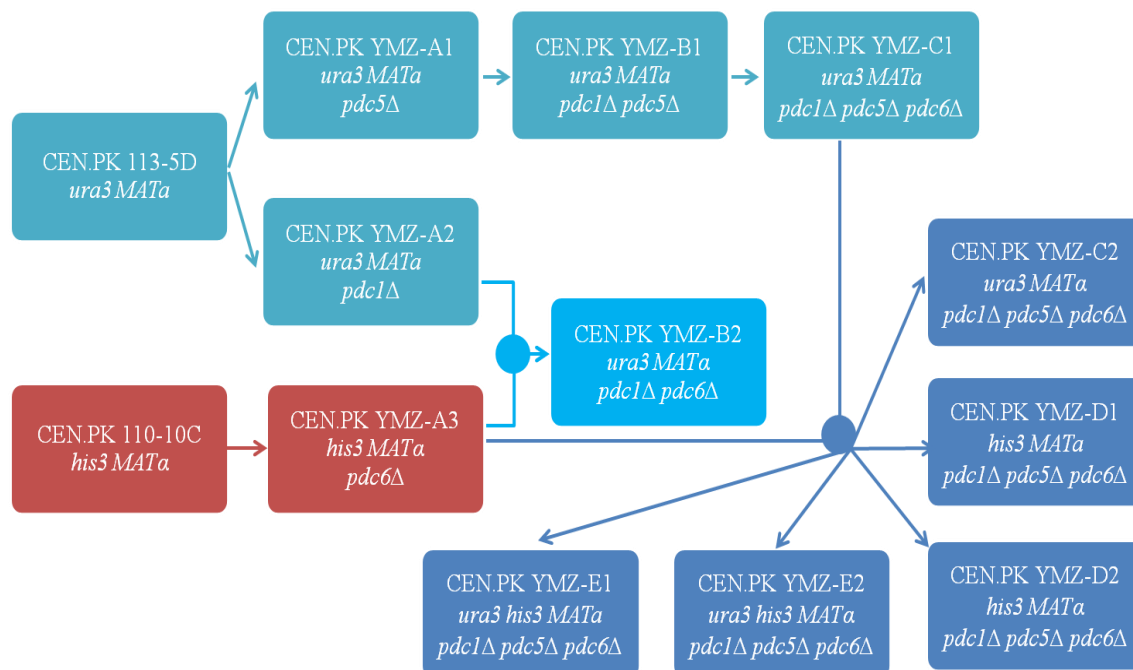


Figure 8. Work flow of Pdc negative strain construction. *PDC1*, *PDC5*, and *PDC6* were consecutively deleted in two different background strains CEN.PK 113-5D (*MATa ura3-52*) and CEN.PK 110-10C (*MATa his3-Δ1*). A collection of Pdc negative strains was obtained using a combination of consecutive deletions with strain crossings and tetrad dissections. The closed circles represent strain crossings.

The adaptive evolution of E1 towards growth on glucose as the sole carbon source was performed in three independent culture lines in 100 mL shake flasks with 20 mL medium at 30 °C, which involved three phases (**Figure 9**).

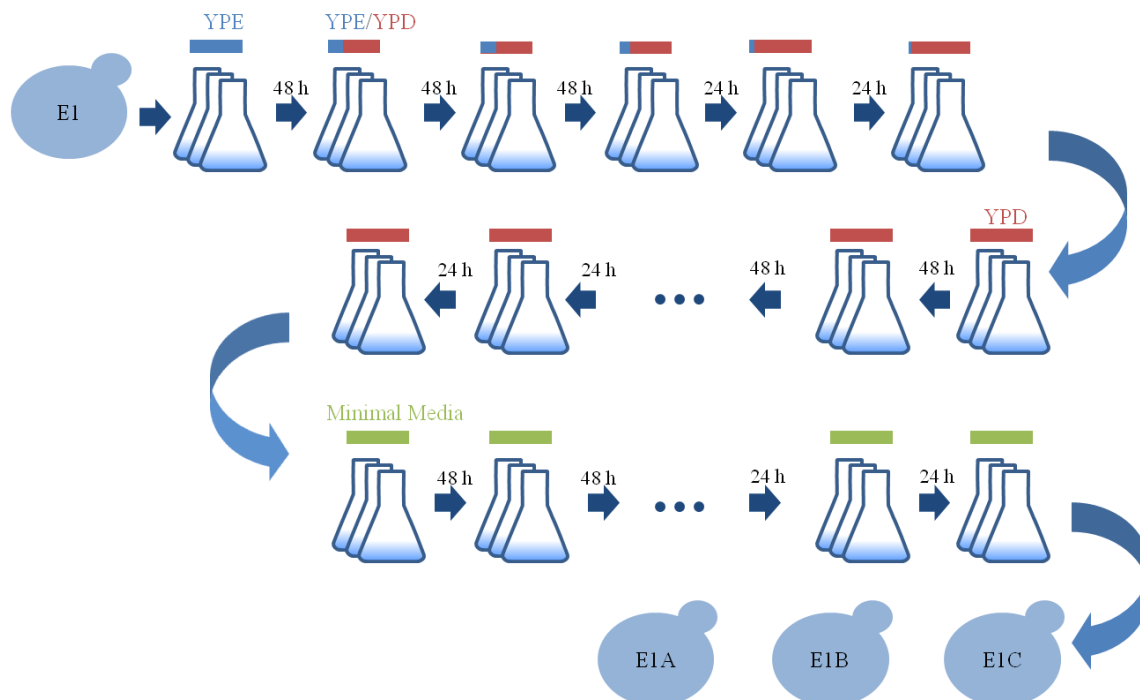


Figure 9. Adaptive evolution process of the Pdc negative strain E1.

First, E1 was evolved in YPD medium with gradually reduced ethanol concentration for glucose tolerance. Then the glucose tolerant strains were further evolved in YPD media for faster growth. Finally the fast-growing and glucose tolerant strains were evolved for C₂ source-independence and faster growth in minimal medium with 2% glucose. The evolved strains were serially transferred every 48 hours or 24 hours. The whole evolution process took 62 days. And three single clones isolates were obtained from the last three shake flasks, respectively, which were designated as CEN.PK YMZ-E1A, CEN.PK YMZ-E1B, and CEN.PK YMZ-E1C (E1A, E1B, E1C for short, respectively).

The growth of three evolved Pdc negative strains, E1A, E1B and E1C was tested in the minimal medium with 2% glucose as the sole carbon source (data not shown). In the minimal medium, the maximum specific growth rates of E1A, E1B and E1C were 0.138 h⁻¹, 0.148 h⁻¹, 0.141 h⁻¹, respectively.

Cells of the parental Pdc negative strain E1 and its evolved strains (E1A, E1B, E1C) were cultured in YPD media and harvested during exponential phase for genomic DNA extraction. The sequencing was performed multiplexed on an Illumina MiSeq. The raw sequencing data of these strains were filtered and trimmed using protocols as described in [146], and the filtered reads were mapped to the reference genome of a wild type strain CEN.PK 113-7D.

The genome sequencing results (**Table 1**) identified three SNVs (Single Nucleotide Variants) in coding regions representing nonsynonymous mutations in the E1A strain; 11 SNVs in coding regions representing nonsynonymous mutations in the E1B strain; and 6 SNVs in coding regions representing nonsynonymous mutations, one chromosomal regional deletion, one mitochondrial regional deletion and one single nucleotide insertion in the E1C strain. Among all genes with SNVs, three genes, *MTH1*, *HXT2* and *CIT1*, were found to carry point mutations in all three evolved strains. And another gene, *RPD3*, was found to carry point mutations in two of the evolved strains. *MTH1* encodes a negative regulator of the glucose-sensing signal transduction pathway, as described before. *HXT2* encodes a high-affinity glucose transporter, which is usually found to function under low glucose concentrations and its transcription is repressed by high glucose and induced by low glucose [147, 148]. *CIT1* encodes a mitochondrial citrate synthase, as reviewed in Chapter 1. *RPD3* encodes a histone deacetylase, which usually functions in the form of a complex together with other proteins to regulate gene transcription, silencing and many other processes by histone deacetylation [149-151].

Table 1. Point mutations in evolved Pdc negative strains.

Chr	Position	E1	E1A	E1B	E1C	Nucleotide change	Effect	Gene(s)	Amino acid change	Codon change	Codon position
MT	62539		// ²		DEL		Deletion of 500-600 bp the gene	chr0_JIGSAW_8452988			
2	548654		//	SNV	A/T		Nonsynonymous	YBR157C	L/I	Tta/Ata	123
4	825268			SNV	A/T		Nonsynonymous	YDR181C	S/T	Tct/Act	375
4	1014480			SNV	A/C		Nonsynonymous	YDR277C	I/S	aTt/aGt	85
4	1014492	12% ¹	SNV	SNV	G/T		Nonsynonymous	YDR277C	A/D	gCt/gAt	81
4	1162017		//		DEL		Deletion of ~1000 bp of gene	YDR345C			
8	435290			SNV	A/G		Upstream: 48 bases Downstream: 200 bases	YHR169W	DBP8		
10	704204			INS	*/+A		Downstream: 359 bases	YJR152W	DAL5		
12	908162			SNV	C/G		Nonsynonymous	YLR401C	DUS3	Gat/Cat	499
13	283022			SNV	G/C		Nonsynonymous	YMR011W	HXT2	Ggt/Cgt	75
13	284197		SNV	SNV	G/A		Novel stop codon	YMR011W		tgG/tgA	466
13	704014			SNV	C/T		Nonsynonymous	YMR219W	ESC1	Ctt/Ttt	736
14	12588		25% ¹		T/C		Nonsynonymous	YNL330C	N/D	Aat/Gat	235
14	12704			SNV	G/A		Nonsynonymous	YNL330C	RPD3	gCg/gTg	196
14	13038			SNV	A/T		Nonsynonymous	YNL330C	F/I	Ttt/Att	85
14	278451			SNV	G/C		Nonsynonymous	YNL189W	SRP1	aGc/aCc	73
14	568887		//	SNV	G/T		Nonsynonymous	YNL032W	SIW14	aGc/aTc	132
14	624525		SNV		G/T		Nonsynonymous	YNR001C	P/Q	cCa/cAa	176
14	624528			SNV	T/C		Nonsynonymous	YNR001C	H/R	cAt/cGt	175
14	624802		//	SNV	T/C		Nonsynonymous	YNR001C	M/V	Atg/Gtg	84
14	742966		//	SNV	C/A		Downstream: 150 bases	YNR064C, YNR063W			
16	469045		//	SNV	G/T		Downstream: 220 bases	YPL045W	VPS16	V/F	617
				SNV	G/T		Nonsynonymous			Gtt/Ttt	

¹: The value means the percentage reads of the mutations, ideally representing the percentage of the sequenced cells. And the mutation was excluded after sequencing of the individual gene. ²: Unfixed mutations.

Interestingly, two identical mutations occurred in more than one strain, A81D in *Mth1* and W466* in *Hxt2*, and two mutations affected adjacent amino acids, P176Q and H175R in *Cit1*.

The most interesting gene is *MTH1*, since several other *MTH1* alleles have been identified in selections of glucose or catabolite repression suppressors using glucose sensitive mutants besides *MTH1-ΔT* [111-115]. Among these *MTH1* alleles affecting glucose sensing, e.g. *BPC1-1*, *DGT1-1*, *HTR1-5*, *HTR1-19* and *HTR1-23*, two mutations in codon 85 (I85N, I85S) and one mutation in codon 102 (S102/G) were identified. It was found that both mutations in codon 85 could alleviate glucose repression and that the S102G mutation could reinforce the mutations in codon 85 although having no effects by itself [113, 114]. Since the mutation I85S has already been confirmed to suppress glucose repression, the mutation A81D was chosen to be validated through reverse engineering in this study, to investigate if it has similar effects like other mutations.

To introduce the mutation A81D in *MTH1*, an *MTH1^{81D}* construct was created and used to replace the native *MTH1* in the parental Pdc negative strain E1, as shown in **Figure 11**, yielding two M81 transformants, M81-11 and M81-33. They were tested for growth in glucose minimal medium. Their growth profiles in minimal medium with 2 % glucose are shown in **Figure 11**, with the maximum specific growth rates of 0.053 h⁻¹ and 0.047 h⁻¹, respectively.

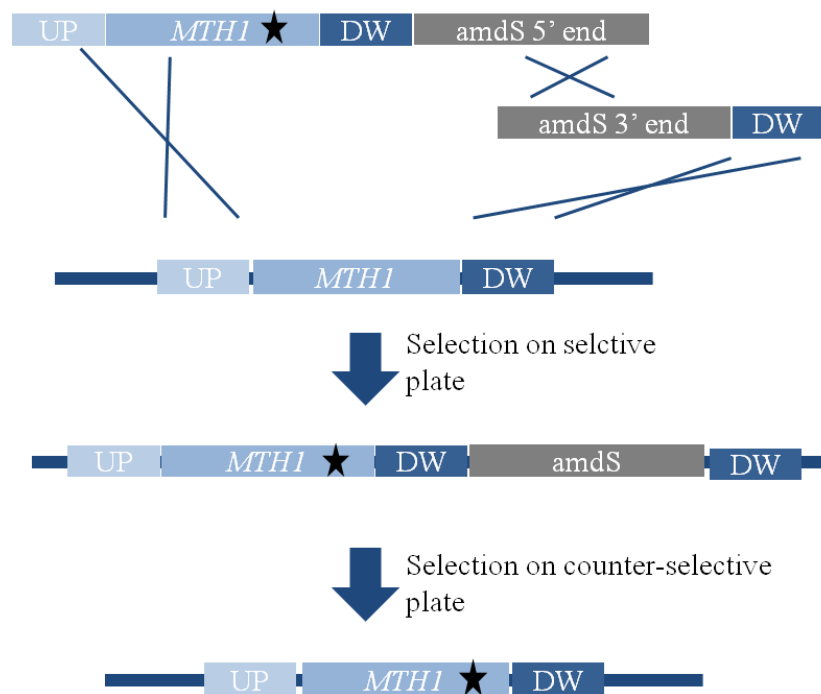


Figure 10. Reverse engineering strategy for *MTH1^{81D}* integration into *MTH1* locus of the E1 strain.

The fact that *MTH1*^{81D} by itself could restore growth of the Pdc negative strain on glucose suggested its similar effects on glucose repression alleviation [108, 111-115]. However, the maximum specific growth rates were smaller than those of the evolved strains E1A, E1B, E1C. The *MTH1*^{81D} mutation contributes around 35% of the specific growth rate in the evolved E1 strains, indicating that other genetic changes are likely to contribute to the growth recovery as well.

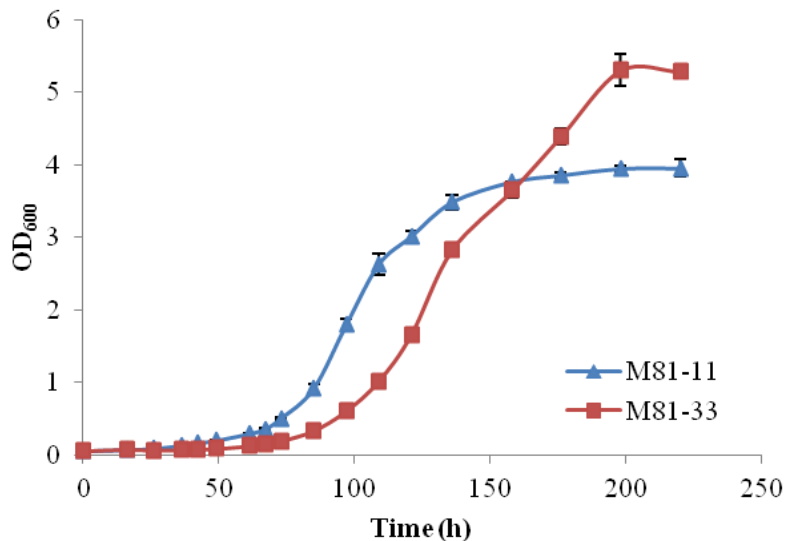


Figure 11. Growth profiles of reverse engineered strains M81-11 and M81-33 (two transformants, *ura3-52 his3-Δ1 pdc1Δ pdc5Δ pdc6Δ mth1::MTH1*^{81D}) in minimal medium with 2% glucose. All measurements are mean +/- standard error of three biological replicates.

In order to understand the effects of the *MTH1*^{81D} allele on transcription of hexose transporter genes, transcription analysis was performed on *HXT1-7* using qPCR in reverse engineered strains M81-11 and M81-33 and a wild type strain CEN.PK 113-11C [138]. Cells for RNA extraction were cultured in minimal medium and harvested during exponential growth phase (OD₆₀₀ ~1). *ACT1*, a housekeeping gene, was selected as the reference gene [152]. Since *HXT6* and *HXT7* have nearly identical sequences, they used the same pair of primers for qPCR. Therefore, the transcription analysis result for *HXT6* and *HXT7* was their sum-up.

Compared with the wild type, the expression levels of *HXT1*, *HXT3*, *HXT4* and *HXT6&7* were much lower in both M81 transformants, *i.e.* around 9 fold, 25 fold, 15 fold, and 40 fold lower, respectively (**Figure 12**). The expression level of *HXT5* did not show much difference in the M81 strains and the wild type, around 1.5 fold higher in the M81 strains. However, the expression level of *HXT2* was much higher in the M81 strains, *i.e.* around 3 fold higher, a different pattern from other *HXTs*. The different expression patterns of *HXTs* in M81 strains suggested that they were regulated by Mth1 in different ways.

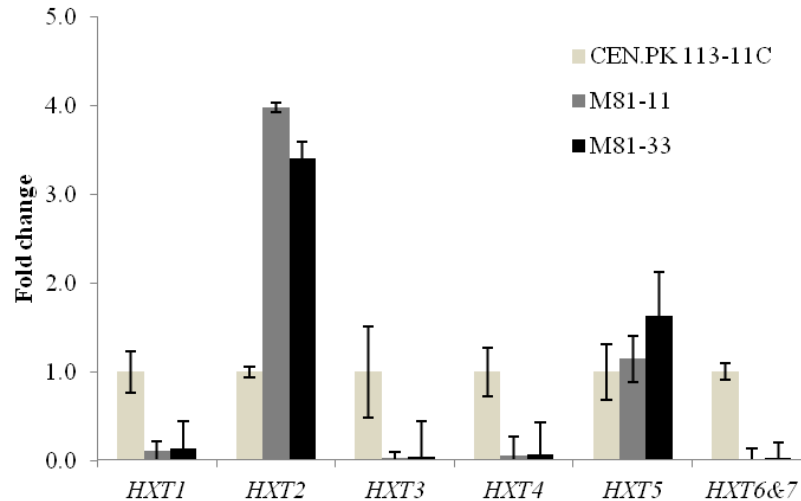


Figure 12. Transcription analysis of *HXTs* (*HXT1-7*) in two M81 strains and wild type strain CEN.PK 113-11C. The transcription levels of *HXTs* in CEN.PK 113-11C are set at 1. All measurements are mean \pm standard error of three biological replicates.

In addition, a bioinformatics approach was undertaken to gain sequence-function insight into these mutations in the four proteins. Homologous sequences were queried using the basic local alignment search tool (BLAST) of NCBI database, and then were filtered to retain only those with identity of 40% ~ 95% to the *S. cerevisiae* enzymes to reduce bias. The remaining sequences were aligned using MUSCLE [153], and the resulting alignments were used to compute the conservation of each amino acid in the *S. cerevisiae* proteins compared to the filtered BLAST results. The conservation values were used to color-code sequence representations of the *S. cerevisiae* proteins, as shown in **Figure 13**. Homology models were generated for three of the four proteins using the Swiss-Model repository [154], with the aim of gaining insights into the function of the mutations, as shown in **Figure 14**.

The BLAST search performed with Mth1 from *S. cerevisiae* yielded only 22 homologous sequences after filtering, which were orthologs of Mth1 or its homolog Std1 from unicellular fungi. Both A81 and I85 are conserved in 21 out of the 22 analyzed sequences, And A81 and I85 are positioned on an ‘island’ composed of 22 highly conserved amino acids from codon 71-91 (**Figure 13A**). The high degree of conservation of this region indicates functional or structural importance for the protein function, like the other conserved ‘island’ from codon 118 to 137 (**Figure 13A**), which is the identified target region for phosphorylation by Yck1 [116]. Since no protein crystal structures of Mth1 or homologs are available, predictions were performed for the secondary structure of the conserved ‘island’ (codon 71-91) using four prediction tools [155] (**Figure 15A**), which all indicated an alpha helix formed in this region (**Figure 15B**). The putative helix is likely initiated by the structurally rigid prolines at codon 74 and 75. Predictions for which

amino acids are exposed to the solvent and which are buried were also generated using two different tools, and both tools used predict Y77, A81, I85 and L89 to be buried away from the solvent [156] (**Figure 15A**). A helical-wheel representation was generated using the amino acids predicted to form an alpha helix (residues 75-89) (**Figure 15B**). The aim was to examine the topology of the predicted alpha-helix. The helical-wheel representation shows an amphipathic alpha helix with the buried residues Y77, A81, I85 and L89 on one side, whereas the opposite side solely has acidic and basic residues. Therefore, it is proposed that A81 and I85, together with Y77 and L89, play a structural role in anchoring a highly conserved alpha helix to the Mth1 surface via hydrophobic interactions. The A81D, I85S or I85N mutations, representing changes from non-polar to polar amino acids, would disrupt their interactions and may therefore change the secondary structure. Since the two conserved ‘islands’ are 27 residues apart, it is reasonable to speculate that the putative helix may interact with the phosphorylation site, and thus affect the Mth1 degradation [148].

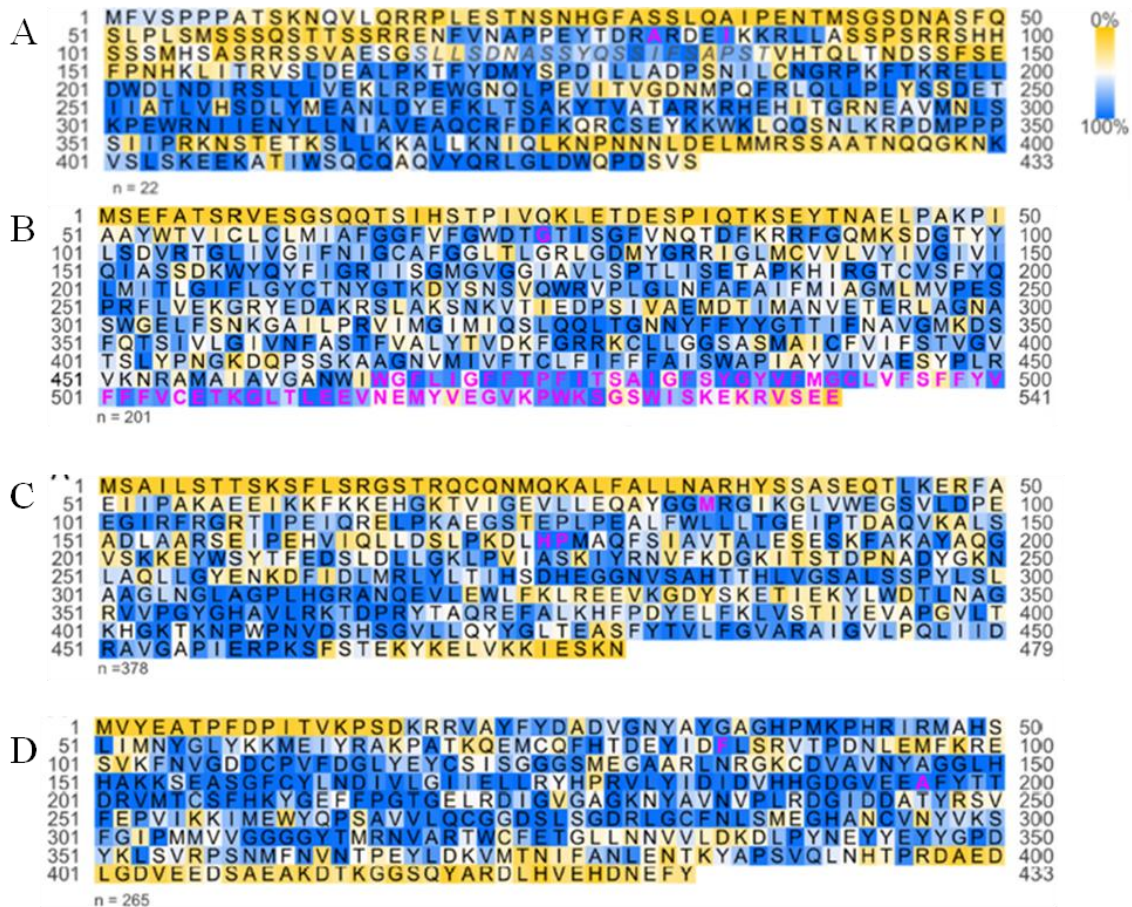


Figure 13. Mapping and analysis of mutations in Mth1 (A), Hxt2 (B), Cit1 (C) and Rpd3 (D). The protein sequences of *S. cerevisiae* are shown with colored conservation levels. Yellow indicates low conservation, white intermediate, and blue high. Magenta text indicates positions for non-synonymous mutations identified in this study. n presents the number of homologous sequences used in a multiple alignment. A) Gray and italic text indicates the phosphorylation region of casein kinase Yck1.

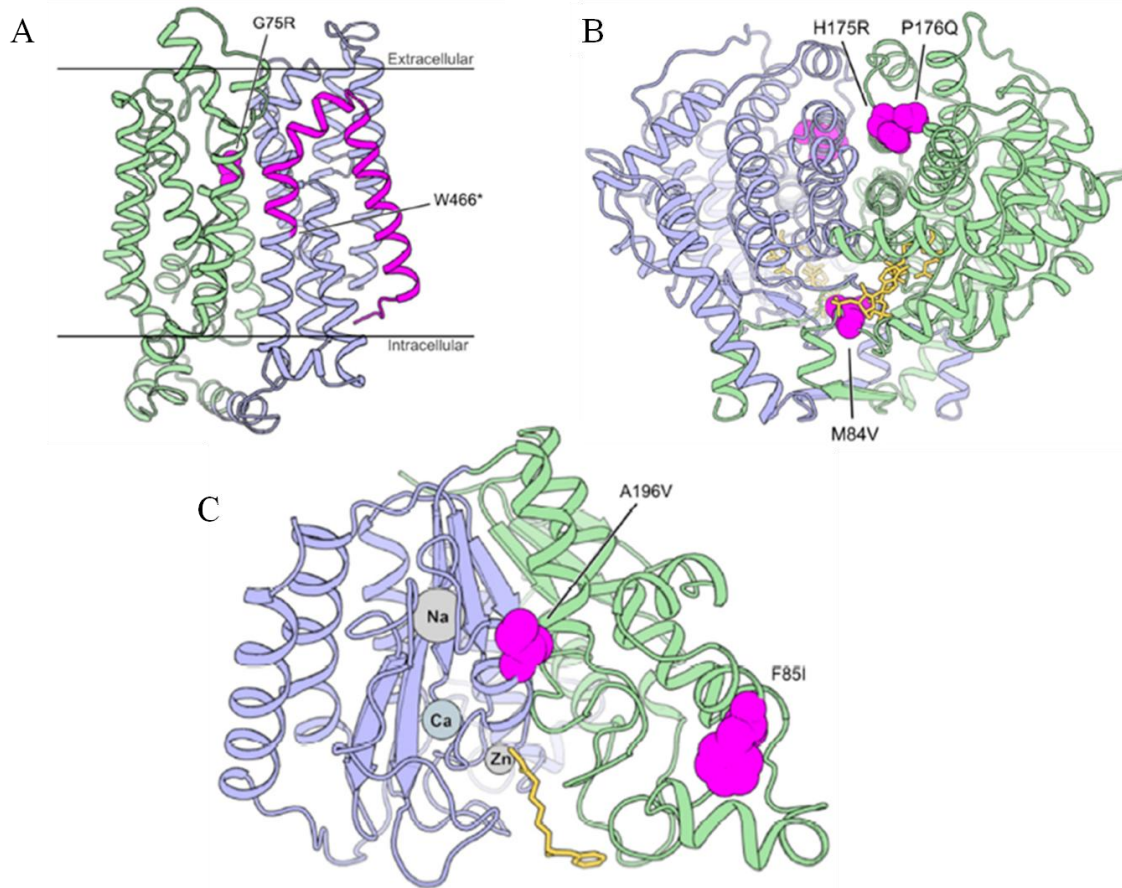


Figure 14. A cartoon representation of homology protein models generated for Hxt2 (A), Cit1 (B) and Rpd3 (C). A) An Hxt2 homology model generated using the crystal structure of the human glucose transporter Glut1 (PDB ID: 4PYP). The N-terminal and C-terminal domain of the peptide are shown in pale green and purple, respectively. The global position of the mutation G75R is indicated by magenta sphere representation, and the mutation W466* by magenta coloring for the deleted protein sequence. Lines indicate the approximate boundaries of the phospholipid bilayer in which the protein performs its function. B) A Cit1 homology model generated using a crystal structure of chicken citrate synthase (PDB ID: 1AL6). The position of mutations is indicated by magenta sphere representations of the amino acids in the two polypeptides of the Cit1 homodimer shown in pale purple and pale green, respectively. The substrate oxaloacetate and the substrate analog N-hydroxyamido-CoA are shown in yellow. C) A Rpd3 homology model generated using a crystal structure of the human histone deacetylase 2 protein (PDB: 4LXZ). The N-terminal and C-terminal domain of the polypeptide are shown in pale green and pale purple, respectively. The global position of mutations is indicated by magenta sphere representations of the amino acids. The enzyme inhibitor Vorinostat co-crystallized with the enzyme is shown in yellow. Metal ions in the structure are shown in grey colors (Na: sodium ion, Ca: calcium ion; Zn: zinc ion.).

The BLAST search performed with Hxt2 resulted in 201 sequences after filtering, which come exclusively from unicellular fungi. In this dataset the G75 position is completely conserved and W466 is also highly conserved at 93% (**Figure 13B**). Furthermore in the W466* mutant there are many amino acids with close to complete conservation that are missing due to the premature stop codon (**Figure 13B**). A homology model of Hxt2 was generated using the human glucose transporter Glut1 [157] (**Figure 14A**). G75 is positioned in the interface between the N- and C-terminal domains, with the alpha carbon facing inwards in a bundle of four helices that form the substrate channel. W466 and the

The BLAST search performed with Rpd3 resulted in 265 sequences after filtering, which come from unicellular and multicellular fungi, plants, animals and a range of bacteria. Analysis of these sequences revealed that the F85 position is 97% conserved and the A196 position is 98% conserved (**Figure 13D**). A homology model of Rpd3 was generated using the crystal structure of the human histone deacetylase 2 protein (**Figure 14C**). F85 is buried in between two alpha helices and a loop in the N-terminal domain, with less conserved surrounding residues. The conservation data and properties of the amino acids in this region indicate that F85 is important for the hydrophobic packing of this region and thus serves a structural role in the protein. A196 is part of an alpha helix that is situated at the interface between the N- and C-terminal domains, which is highly a conserved region. The residues are obviously very sensitive to mutations. It is possible that the two extra methyl groups introduced by the A196V mutation may cause a displacement of the conserved helix and result in decreased or abolished enzyme activity.

Based on the results and the predictions above, some possible mechanisms were proposed for the evolved Pdc negative strains.

In an unevolved Pdc negative strain, although Ach1 could channel acetyl-CoA from the mitochondria to the cytosol, it is only functional under glucose derepressed conditions. And this route can be blocked by the limited mitochondria acetyl-CoA due to the stringent regulation in *S. cerevisiae* (**Figure 16A**), e.g. the regulated activity of the PDH complex via the post-transcriptional phosphorylation of Pda1 subunits [28] or the transcriptional repression of Lpd1 subunits [27].

In the evolved Pdc negative strains, the mutations in Mth1 seemed to play the most critical role, since the allele with a single mutation *MTH1*^{81D} alone has been proved to restore the growth of the Pdc negative strain on glucose, as well as *MTH1*- ΔT [108]. According to the predictions of the conserved 'island' (codon 71-91) in Mth1, A81 and I85 may play a structural role in maintaining the putative alpha helix formed within it, and thus the mutations on either site probably affect the phosphorylation region of Yck1 in another adjacent conserved 'island'. However, a crystal structure of Mth1 would be instrumental to validate these predictions. The *MTH1* alleles seem to decrease glucose uptake transport by repressing the transcription of several *HXTs* (**Figure 12**) [111, 112, 114, 115], which was also observed in the TAM strain by van Maris *et al* [107]. Moreover, a regional deletion within *HXT3* (~1000 bp) in an evolved strain E1C would undoubtedly destroy its activity to transport glucose. A previous study suggested that the rate of glucose transport determines the strength of glucose repression [158]. With the reduced glucose uptake, the transcription of many glucose repressed genes, e.g. those encoding mitochondrial enzymes, could probably be partially derepressed despite the high extracellular glucose. Therefore, in the evolved Pdc negative strains with the

mutations in *MTH1*, it is possible that the cytosolic acetyl-CoA supply shuttled from the mitochondria via Ach1 route was no longer blocked (**Figure 16B**).

The mutations in *HXT2* seemed to make no sense in high glucose medium (2% glucose) used in this study, since its expression is usually induced by low glucose and repressed by high glucose [147, 159]. One possible explanation would be the possible complicated effects of the mutated Mth1. Transcriptional analysis of the TAM strain showed decreased transcription of *HXT1*, *HXT3*, *HXT4*, *HXT6* and *HXT7*, and increased transcription of *HXT2* and *HXT5* [107], which is consistent with our qPCR results (**Figure 12**). The mutations in Hxt2 might result in structural disruptions based on our predictions, and may therefore further reduce glucose transport in this strain.

The mutations in *CIT1* might also be connected with cytosolic acetyl-CoA supply via the Ach1 route. As shown in **Figure 16B**, Cit1 competes with Ach1 for the substrate acetyl-CoA in the mitochondria. The mutated Cit1 with potentially decreased activity, as predicted by the bioinformatics analysis of the identified mutations, might allow for more acetyl-CoA being converted to acetate by Ach1, and would therefore provide more acetate for cytosolic acetyl-CoA biosynthesis. The previous study on Ach1 suggested that C₂ supply in the cytosol seemed to be a limiting step for the growth of Pdc negative strains. Thus, the Cit1 mutations might further improve growth on glucose in the presence of the mutated Mth1. However, when *CIT1* was disrupted in the strain M81, the growth on glucose was significantly impaired (data not shown), since the complete disruption of *CIT1* would result in the dysfunction of the TCA cycle and hereby significantly reduce the ability to generate ATP required for growth.

Although the Rpd3 mutations were predicted to result in activity decreases, it is still too difficult to speculate about their roles in the evolved Pdc negative strains, since more and more studies suggest that histone acetylation and deacetylation regulate gene transcription in complex and comprehensive ways [160]. A previous study found that histone acetylation and deacetylation was directly related with nucleocytosolic acetyl-CoA abundance [19]. One possible speculation would be that the mutations in Rpd3 might be related to cytosolic acetyl-CoA abundance as well, but this will require further investigation.

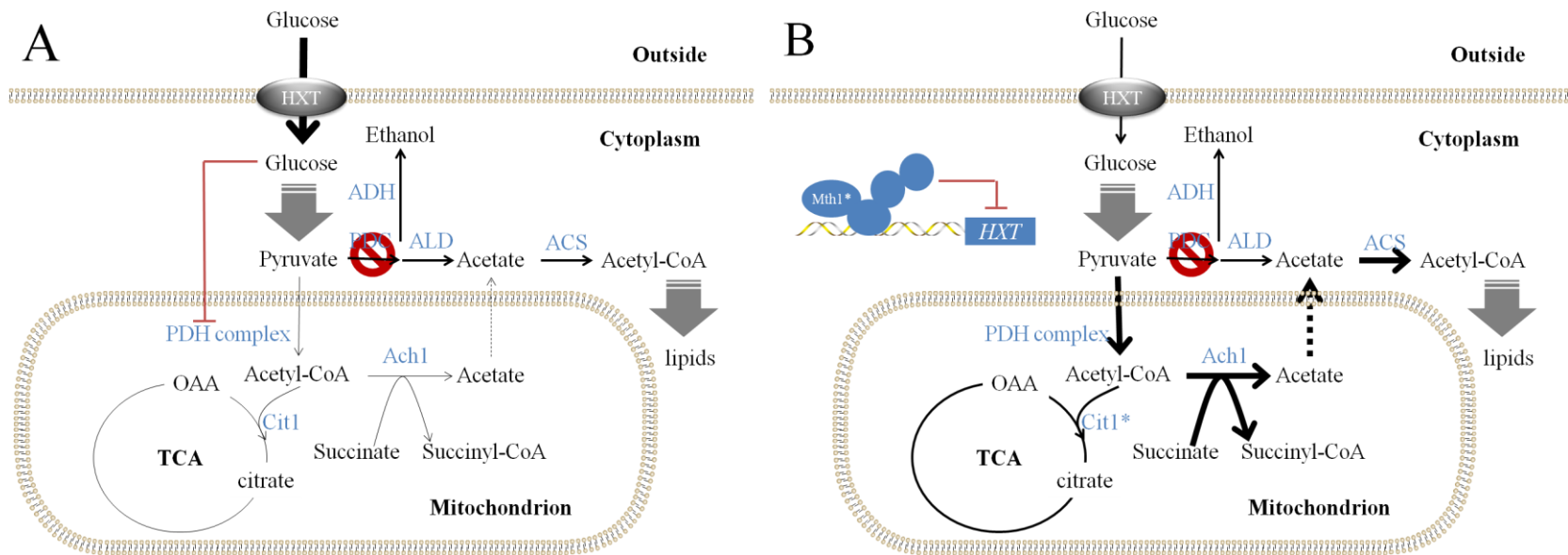


Figure 16. A simple illustration for the possible roles of the mutated proteins in the evolved *pdc* negative strains. The solid arrows represent the reactions catalyzed by the enzymes, which are indicated in blue text. The dash line represents the transportation between different subcellular organelles. The red lines with a bar at one end represent the repression or inhibition. The red circles represent the block due to *PDC* deletions. A) Simplified acetyl-CoA metabolism in the parental *Pdc* negative strain. The PDH complex and TCA cycle enzymes is repressed by high glucose uptake via hexose transporters (HXTs). B) Simplified acetyl-CoA metabolism in evolved *Pdc* negative strains with point mutated *Mth1* (*Mth1**) and *Cit1* (*Cit1**). Glucose uptake via HXT decreases in the presence of *Mth1**, resulting in derepression of the PDH complex and TCA cycle enzymes. *Cit1** with predicted decreased activity allows more mitochondria acetyl-CoA convert to acetate by *Ach1*, which can be transported to the cytosol and converted to acetyl-CoA there.

3.3 Functional bacterial pyruvate formate lyase expressed in a Pdc negative strain

Pdc negative strains can serve as potential non-ethanol producing platform strains for biochemical production. However, they cannot grow on glucose as the sole carbon source. Although *MTH1-ΔT* can restore its growth on glucose, its capacity for glucose consumption is limited as well as the cytosolic acetyl-CoA supply. In order to increase cytosolic acetyl-CoA supply in IMI076, an alternate synthetic pathway, pyruvate formate lyase (PFL) pathway from *E. coli*, was introduced to convert pyruvate to acetyl-CoA in the cytosol.

The PFL is activated by its activating enzyme PFL-AE with two other cofactors (or co-substrates), reduced flavodoxin and S-adenosylmethionine (SAM) [161]. The PFL-AE uses reduced flavodoxin as an electron donor and SAM as a co-substrate to generate a free radical (5^{\cdot} -dA \cdot) for PFL activation [162]. In an *in vitro* study it was found that other artificial one-electron reductants can also serve as the electron donor for the PFL pathway [163]. Functional PFL pathway from *E. coli* and *Lactobacillus plantarum* has been expressed in yeast under anaerobic conditions [16, 164]. Waks and Silver coexpressed *pflA* (PFL gene) and *pflB* (PFL activating enzyme gene) in a strain with deletions in both formate dehydrogenase (FDH) genes, *FDH1* and *FDH2*, which increased formate production by 4.5 fold under anaerobic conditions [164]. Kozak *et al.* found that *pflA* and *pflB* co-expression could restore growth of an ACS deficient (*acs1Δ acs2Δ*) mutant on glucose under anaerobic conditions, by complementing cytosolic acetyl-CoA synthesis [16]. In these studies the cofactors were, however, not co-expressed even though it was speculated that there could be other cytosolic, single-electron donors replacing reduced flavodoxin to activate PFL [164].

In this study, the PFL pathway (encoded by *pflA* and *pflB*) was expressed in IMI076, or with two different cofactors and their reductase (*fdx-fpr*, *fldA-fpr*). We found that the co-expressed cofactors, especially *fldA-fpr*, facilitates the PFL pathway function at aerobic growth conditions, which could be useful for its application in yeast bioprocesses that have to be operated at aerobic conditions.

pflA and *pflB* from *E. coli* were codon-optimized for expression in *S. cerevisiae*, and cloned under the control of the constitutive promoters P_{PGK1} and P_{TEF1} respectively into the vector pSP-GM1 [139], yielding pPFL01. pSP-GM1 and pPFL01 were transformed into the background strain IMI076 respectively, yielding YZ10 and YZ11. Two transformants of each strains were picked and cultured in glucose minimal medium at aerobic growth conditions using Bioscreen C. Growth results revealed that, two YZ11 transformants (with the PFL pathway) reached a higher final biomass, compared with two YZ10 transformants (without the PFL pathway) (**Figure 17A**). No major growth difference was observed between different transformants for both strains. The growth of YZ10-1 and YZ11-1 was further confirmed by culturing in shake flasks, as shown in **Figure 17B**. However, a small improvement in final biomass concentration was observed with the PFL pathway expressed (**Figure 17**). As reported by *in vitro* studies, the activated PFL is

sensitive to oxygen and it cleaves into fragments at the activation site when exposed to oxygen [165]. Therefore, the function of the PFL pathway with constitutive expression was limited under aerobic conditions, which may explain the small increase in the final biomass concentration.

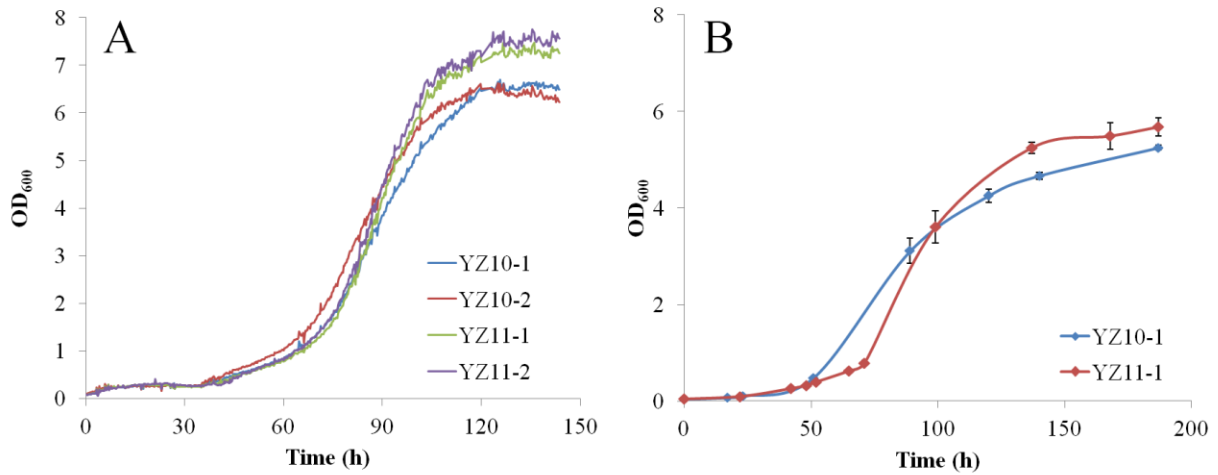


Figure 17. Growth comparisons of the strains with and without the PFL pathway in minimal medium using Bioscreen C (A) and shake flasks (B). A) Two YZ10 transformants YZ10-1 and YZ10-2 (without PFL pathway), and two YZ11 transformants YZ11-1 and YZ11-2 (with PFL pathway) were cultured in octuplicate, and the standard deviations (not shown here) were within 5%. B) YZ10-1 and YZ11-1 were cultured in triplicate in shake flasks.

Two cofactors and their reductase, ferredoxin (encoded by *fdx*) and ferredoxin NADP⁺ reductase (encoded by *fpr*), and flavodoxin (encoded by *fldA*) and flavodoxin NADP⁺ reductase (encoded by *fpr*), were introduced together with the PFL pathway (*pflA* and *pflB*) by being cloned in one plasmid to the background strain IMI076 respectively, resulting in strain YZ12 and YZ13, respectively. Three different transformants of each strain were picked and cultured using minimal medium with 2% glucose in shake flasks, to evaluate the role of the cofactors in the PFL pathway.

As shown in **Figure 18**, all transformants of YZ12 (with PFL pathway and ferredoxin) and YZ13 (with PFL pathway and flavodoxin) reached higher final biomass concentrations, compared with YZ10 (without PFL pathway) and YZ11 (with PFL pathway). However, three transformants of YZ12 and YZ13, respectively, showed different growth behavior. As shown in **Figure 18** and **Table 2**, the three transformants of YZ12 differed from each other in lag phase, maximum specific growth rate and the final biomass concentration, and those of YZ13 differed from each other in the lag phase and the maximum specific growth rate (**Table 2**), but all reached a similar final biomass concentration (**Figure 18B**).

Overall, the transformants with *fldA-fpr* co-expressed showed higher final biomass concentrations than those with *fdx-fpr*, as well as higher specific growth rates in the late growth phase. Moreover, YZ13 transformants consumed all the supplied glucose and accumulated no pyruvate in the culture (**Table 2**). Therefore, reduced flavodoxin seems to be a more efficient cofactor for the PFL pathway than reduced ferredoxin. Although reduced ferredoxin and

flavodoxin can both serve as single electron donors, some enzymes require either one or the other [166, 167]. In *E. coli*, ferredoxin does not substitute for flavodoxin for PFL activation [168], which probably explains why *fdx-fpr* co-expression did not contribute much to biomass formation.

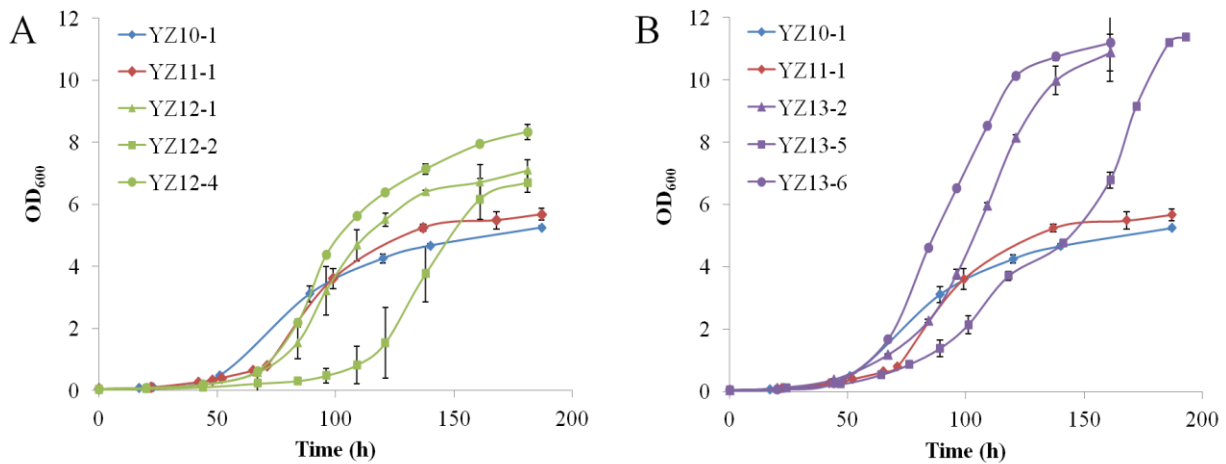


Figure 18. Growth comparisons of YZ10, YZ11, YZ12 and YZ13 in minimal medium using shake flasks. (A) YZ10-1 (without PFL pathway), YZ11-1 (with PFL pathway), and three YZ12 transformants (YZ12-1, YZ12-2, YZ12-4, with PFL pathway and cofactor ferredoxin) ; (B) YZ10, YZ11 and three YZ13 transformants (YZ13-2, YZ13-5, YZ13-6, with PFL pathway and cofactor flavodoxin).

Table 2. Strain properties of YZ10, YZ11, YZ12 and YZ13.

	μ_{\max} (h^{-1})	Y_{Pyr} (g pyruvate / g glucose)	Y_{Gly} (g glycerol / g glucose)	Residual glucose (g/L)	Residual pyruvate (g/L)
YZ10-1	0.055	0.326	0.023	3.97±0.34	3.72±0.04
YZ11-1	0.052	0.316	0.026	2.97±0.10	3.84±0.06
YZ12-1	0.060	0.204	0.021	3.15±0.47	3.22±0.15
YZ12-2	0.052	0.248	0.021	4.06±0.52	3.29±0.02
YZ12-4	0.068	0.255	0.012	2.36±0.07	3.29±0.08
YZ13-2	0.050	0.087	0.025	0.00±0.00	0.00±0.00
YZ13-5	0.045	0.100	0.076	0.00±0.00	0.00±0.00
YZ13-6	0.066	0.108	0.021	0.00±0.00	0.00±0.00

Due to the differences in the growth behavior of the three transformants of each type, we therefore tested gene expression of the four introduced genes via qPCR. Cells for gene expression analysis were cultured in minimal medium and harvested at several different time points during the cultivations. *ACT1* was selected as the reference gene. The results revealed that the expression levels of *pflB* and *pflA* varied up to 2-fold between three YZ12 transformants (**Figure 19A**), and up to 5-fold between three YZ13 transformants (**Figure 19B**). These results indicated that higher expression level of *pflA* or *pflB* might not be beneficial for higher final biomass

concentration. However, YZ13-5 with a relatively low expression of *fldA* showed delayed growth and a higher glycerol yield on glucose. These results suggested that the expression levels of the cofactors might be crucial for optimal function of the PFL pathway under aerobic conditions.

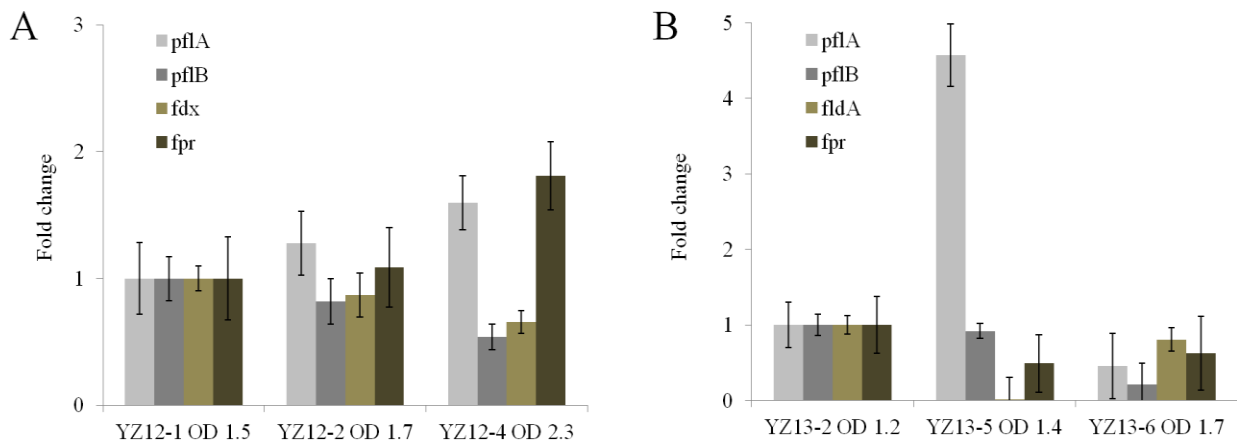


Figure 19 Expression analysis of introduced genes in YZ12 (A) and YZ13 (B). (A) Gene expression analysis of three YZ12 transformants. Samples were taken at OD₆₀₀ between 1-2.5 for the transcription analysis of 4 introduced genes (*pflA*, *pflB*, *fdx*, and *fpr*). The gene expression levels of introduced genes in YZ12-1 were set as 1. (D) Gene expression analysis of three YZ13 transformants. Samples were taken at OD₆₀₀ between 1-2.5 for the transcription analysis of 4 introduced genes (*pflA*, *pflB*, *fldA*, and *fpr*). The gene expression levels of introduced genes in YZ13-2 were set as 1.

However, no formate byproduct was detected at aerobic growth in our study, which was a different observation from that when the PFL pathway was expressed under anaerobic conditions [16, 164]. This might be caused by different activities of FDHs under aerobic and anaerobic conditions, which convert formate to CO₂. In a previous study, it seemed that formate assimilation by FDHs was not as efficient under anaerobic conditions [164] as aerobic conditions [169], probably due to inefficient NAD⁺ recycling in the absence of electron transport chain and oxidative phosphorylation at anaerobic growth. Therefore the transcription levels of *FDH1* and *FDH2* were measured in the different constructed strains, as shown in **Figure 20**. In YZ10-1, the *FDHs* expression levels increased about 5-fold. In YZ11-1, their expression levels increased about 3 fold. In YZ13-2, their expression levels did not increase when OD₆₀₀ increased from 1.2 to 2.3, but increased more than 25 fold when OD₆₀₀ reached 8.1. In YZ13-6, the expression levels increased above 20 fold when the OD₆₀₀ increased from 1.7 to 4.6, and above 15 fold when OD₆₀₀ reached 8.5.

FDHs expression is reported to be induced by methanol or formate, or with glycine as the sole nitrogen source. When the PFL pathway was expressed in an *Acs*⁻ mutant under anaerobic glucose-limited chemostat conditions, the transcript levels of *FDH1* and *FDH2* were over 25-fold higher than those in the wild type [16]. Therefore, the small transcription increase in YZ10-1 and YZ11-1 may result from activities of some unknown reactions related with FDHs [169], whereas the large increase in the two YZ13 transformants probably resulted from a direct response to formate production.

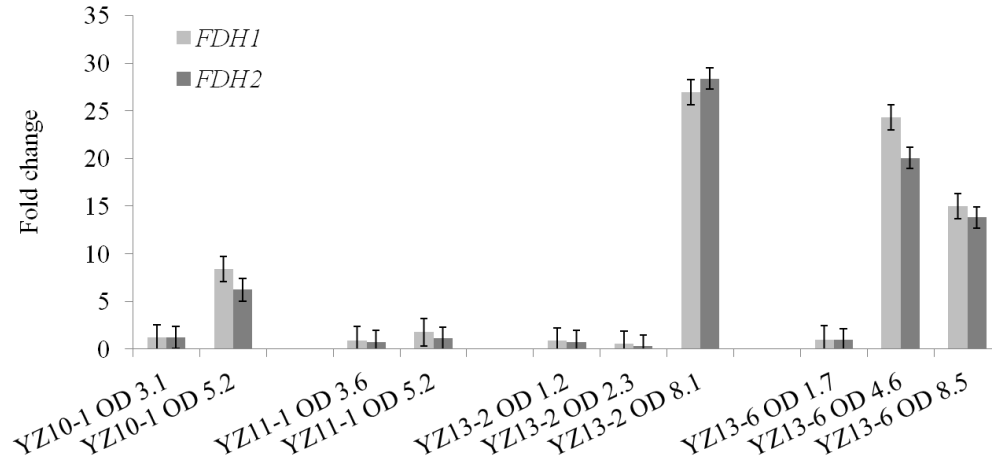


Figure 20. Expression analysis of *FDH1* and *FDH2* in YZ10-1, YZ11-1, YZ13-2 and YZ13-6. *FDH1* and *FDH2* expression levels of YZ13-6 at OD₆₀₀ 1.7 are set to 1.

FDHs expression results suggested that the PFL pathway may function during the late growth phase (OD₆₀₀ above 4), when major induced expression was observed (**Figure 20**). This was consistent with the fact that the PFL pathway with its cofactors mostly contributed to increases in the final biomass concentrations, but not always in the maximum specific growth rates (**Figure 18** and **Table 2**). It indicated that the native pathway (the route via Ach1) provided the cytosolic acetyl-CoA required for growth during the exponential growth phase, while the PFL pathway supplied additional cytosolic acetyl-CoA via pyruvate assimilation. However, it is difficult to explain why it would mainly function during the late growth phase. One hypothesis is that higher cell density in the late growth phase may result in lower dissolved oxygen concentration, which then affected PFL.

Chapter 4. Conclusions and perspective

Yeast serves as a cell factory for production of a wide range of bio-compounds. Acetyl-CoA is an important metabolite as well as precursor for many biochemicals, *e.g.* 1-butanol, PHB, and its cytosolic supply is found to be a limiting factor for synthesis of these bioproducts. Despite many successful strategies for increased cytosolic acetyl-CoA supply, several questions related to cytosolic acetyl-CoA supply remain to be answered. We took the advantage of adaptive laboratory evolution and metabolic engineering, and investigated cytosolic acetyl-CoA supply in a non-ethanol-producing yeast strain. Based on the results and findings presented, we have advanced the understanding of cytosolic acetyl-CoA supply, and could make the following conclusions.

First, the metabolism of acetyl-CoA is highly compartmentalized, and it cannot be directly transported between these subcellular compartments. With help of glyoxylate shuttle, acetyl-CoA produced in the peroxisomes can be shuttled into the cytoplasm or the mitochondria. When carnitine is supplemented into the medium, acetyl-CoA can be transported between the cytoplasm, mitochondria and peroxisomes [77]. However, it was still unclear whether acetyl-CoA generated in the mitochondria can be exported to the cytoplasm without carnitine supplemented. Using a Pdc negative strain IMI076 (Pdc⁻ *MTH1-ΔT ura3-52*), having a reduced glucose uptake rate due to a mutation in the transcriptional regulator Mth1, we identified a route relying on Ach1 that could transfer acetyl units from mitochondria to the cytoplasm in the form of acetate. These results advance the fundamental understanding of acetyl-CoA metabolism in yeast, and could therefore be helpful for construction of yeast cell factories.

Second, with adaptive evolution in glucose medium via serial transfer, three independently evolved strains from a Pdc negative strain were obtained, which were able to grow in minimal medium containing glucose as the sole carbon source at maximum specific rates of 0.138 h⁻¹, 0.148 h⁻¹, 0.141 h⁻¹, respectively. Genome sequencing identified several genetic changes that occurred during the evolution process, among which 4 genes were found to carry point mutations in at least two of the evolved strains: *MTH1*, *HXT2*, *CIT1*, and *RPD3*. Reverse engineering showed that the *MTH1*^{81D} allele is partially responsible for restoring growth of the evolved Pdc negative strains by repressing the total transcriptions of several *HXTs*. The non-synonymous mutations in *HXT2* and *CIT1* may function in the presence of mutated *MTH1* alleles and could be related to the cytosolic acetyl-CoA in a Pdc negative strain. In connection to the Ach1 related acetyl-CoA shuttle route, possible mechanisms were proposed for the generation of acetyl-CoA in evolved Pdc negative strains.

Last but not the least, in connection with establishing a non-ethanol producing yeast platform strain, alternative heterologous pathways can be introduced to increase cytosolic acetyl-CoA supply. In this study, pyruvate formate lyase (PFL) and its activating enzyme from *E. coli* were expressed in a Pdc negative strain, IMI076, as an alternate pathway. PFL is characterized as an enzyme functional at anaerobic conditions, since the radical in the enzyme's active form is sensitive to oxygen. In this study, the PFL pathway was expressed with two different cofactors as

electron donors, ferredoxin or flavodoxin, respectively, and it was found that the co-expression either of these cofactors had a positive effect on growth under aerobic conditions, indicating increased activity of PFL. The positive effect on growth was manifested as a higher final biomass concentration and a significant increase in transcription of formate dehydrogenases (FDHs). Among the two cofactors reduced flavodoxin was found to be a better electron donor than reduced ferredoxin.

Acknowledgments

Looking back on the last four years, I could remember plenty of moments - exciting moments, frustrating moments, joyful moments, painful moments, exhausting moments, relaxing moments; and also people around who shared these happy moments together as well as helped me through those hard moments.

With that, first of all, I would like to sincerely thank my supervisor, Professor Jens Nielsen, for offering me this opportunity to be part of the big Sys²Bio family, giving valuable suggestions and freedom on my project, and encouraging and supporting me along the four years. His great expertise, inspiring smiles, optimistic attitudes, unbelievable efficiencies, open minded instructions are crucial for the accomplishment of my thesis. Jens, thank you very much for all your support, instructions, patience, encouragements, and suggestions along the way. What I learned from you are precise treasures for life.

My great gratitude also goes to my co-supervisors, Dr Verena Siewers and Dr. Anastasia Krivoruchko, for giving me their professional and detailed instructions, which helped to grow as a young scientists. Thank you, Verena and Anastasia, you were always there when I needed trouble-shootings. And a special acknowledgment goes to Dr Yun Chen, for inspiring discussions and great efforts to the project.

I would like to acknowledge my close collaborators, Dr Martin KM Engqvist, Dr. Björn M Hallström, Dr. Lifang Liu, Dr Zongjie Dai for their productive discussions and contributions to the project. And Professor Christer Larsson, Professor Ivan Mijakovic, Associate Professor Dina Petranovic, and Docent Joakim Norbeck are also thanked for their excellent comments in the seminars.

I would like to thank all of the administrators and research engineers, Erica Dahlin, Helena Janveden, Martina Butorac, Anna Bolling, Marie Nordqvist, Ximena Roza Sevilla, Malin Nordvall, Suwane Jansa-Ard, Emma Ribbenhed, Julia Karlsson, Andreas Hellström for their professional assistance in the office and in the lab.

In addition to the people mentioned above, I also would like to acknowledge many close colleagues and friends for their help and accompany. Ik-Kwon Kim, Jin Hou, Xin Chen, Mingtao Huang, Rahul Kumar, Yongji Zhou, Klaas Buijs, Guodong Liu, Jichen Bao, Yating Hu, Bouke de Jong, Shuobo Shi, David Julleson, Mingji Li, Juan Valle, Cheng Zhang, Mark Bisschops, Jiufu Qin, Abderahmane Derouiche, Eugene Fletcher, Zhiwei Zhu, Michael Gossing, Ruifei Wang, Sterfan Tippmann, Lei Shi, Min-Kyoung Kang, Boyang Ji, Paulo Teixeira, Yongjun Wei, Clara Navarrete, Florin David, Zihe Liu, Hülya Karaca Gençer, Eduard Kerkhoven, Petri-Jaan Lahtvee, JoséL. Martínez, Payam Ghiaci, Nina Johansson, Tao Yu, Luis Caspeta-Guadarrama, Kanokarn Kocharin and all of you in sysbio group, thank you very much for being around and always supportive.

A special acknowledgement goes to China Scholarship Council and my domestic responsibility supervisor Professor Ju Chu, for their support, caring, advices and encouragements since I planned my PhD study.

Finally, I own my deepest gratitude to my families, my parents and grandparents, for their forever and unconditional love and support. And thanks my boyfriend for being there with all my moods.

References

1. Nielsen, J., et al., *Metabolic engineering of yeast for production of fuels and chemicals*. Curr Opin Biotechnol, 2013. **24**(3): p. 398-404.
2. Nielsen, J. and M.C. Jewett, *Impact of systems biology on metabolic engineering of Saccharomyces cerevisiae*. FEMS Yeast Res, 2008. **8**(1): p. 122-31.
3. Hong, K.K. and J. Nielsen, *Metabolic engineering of Saccharomyces cerevisiae: a key cell factory platform for future biorefineries*. Cell Mol Life Sci, 2012. **69**(16): p. 2671-90.
4. Nielsen, J., et al., *Engineering synergy in biotechnology*. Nat Chem Biol, 2014. **10**(5): p. 319-22.
5. Chen, Y. and J. Nielsen, *Advances in metabolic pathway and strain engineering paving the way for sustainable production of chemical building blocks*. Curr Opin Biotechnol, 2013. **24**(6): p. 965-72.
6. Nielsen, J., *Synthetic biology for engineering acetyl coenzyme a metabolism in yeast*. MBio, 2014. **5**(6).
7. Krivoruchko, A., et al., *Microbial acetyl-CoA metabolism and metabolic engineering*. Metab Eng, 2014. **28C**(0): p. 28-42.
8. Shiba, Y., et al., *Engineering of the pyruvate dehydrogenase bypass in Saccharomyces cerevisiae for high-level production of isoprenoids*. Metab Eng, 2007. **9**(2): p. 160-8.
9. Chen, Y., et al., *Establishing a platform cell factory through engineering of yeast acetyl-CoA metabolism*. Metabolic Engineering, 2013. **15**: p. 48-54.
10. Chen, Y., V. Siewers, and J. Nielsen, *Profiling of Cytosolic and Peroxisomal Acetyl-CoA Metabolism in Saccharomyces cerevisiae*. PLoS One, 2012. **7**(8).
11. Krivoruchko, A., et al., *Improving biobutanol production in engineered Saccharomyces cerevisiae by manipulation of acetyl-CoA metabolism*. Journal of Industrial Microbiology & Biotechnology, 2013. **40**(9): p. 1051-1056.
12. Kocharin, K., et al., *Engineering of acetyl-CoA metabolism for the improved production of polyhydroxybutyrate in Saccharomyces cerevisiae*. AMB Express, 2012. **2**(1): p. 52.
13. de Jong, B.W., et al., *Improved production of fatty acid ethyl esters in Saccharomyces cerevisiae through up-regulation of the ethanol degradation pathway and expression of the heterologous phosphoketolase pathway*. Microb Cell Fact, 2014. **13**(1): p. 39.
14. Papini, M., et al., *Physiological characterization of recombinant Saccharomyces cerevisiae expressing the Aspergillus nidulans phosphoketolase pathway: validation of activity through ¹³C-based metabolic flux analysis*. Appl Microbiol Biotechnol, 2012. **95**(4): p. 1001-10.
15. Kocharin, K., V. Siewers, and J. Nielsen, *Improved polyhydroxybutyrate production by Saccharomyces cerevisiae through the use of the phosphoketolase pathway*. Biotechnol Bioeng, 2013. **110**(8): p. 2216-24.
16. Kozak, B.U., et al., *Replacement of the Saccharomyces cerevisiae acetyl-CoA synthetases by alternative pathways for cytosolic acetyl-CoA synthesis*. Metab Eng, 2014. **21**: p. 46-59.
17. Lian, J., et al., *Design and construction of acetyl-CoA overproducing Saccharomyces cerevisiae strains*. Metab Eng, 2014. **24**: p. 139-49.
18. Kozak, B.U., et al., *Engineering Acetyl Coenzyme A Supply: Functional Expression of a Bacterial Pyruvate Dehydrogenase Complex in the Cytosol of Saccharomyces cerevisiae*. MBio, 2014. **5**(5).
19. Takahashi, H., et al., *Nucleocytosolic acetyl-coenzyme A synthetase is required for histone acetylation and global transcription*. Molecular Cell, 2006. **23**(2): p. 207-217.
20. Suissa, M., K. Suda, and G. Schatz, *Isolation of the nuclear yeast genes for citrate synthase and fifteen other mitochondrial proteins by a new screening method*. EMBO J, 1984. **3**(8): p. 1773-81.
21. Jia, Y.K., A.M. Becam, and C.J. Herbert, *The CIT3 gene of Saccharomyces cerevisiae encodes a second mitochondrial isoform of citrate synthase*. Mol Microbiol, 1997. **24**(1): p. 53-9.
22. Hartig, A., et al., *Differentially regulated malate synthase genes participate in carbon and nitrogen metabolism of S. cerevisiae*. Nucleic Acids Res, 1992. **20**(21): p. 5677-86.
23. Stoops, J.K., et al., *On the unique structural organization of the Saccharomyces cerevisiae pyruvate dehydrogenase complex*. J Biol Chem, 1997. **272**(9): p. 5757-64.
24. Stoops, J.K., et al., *Three-dimensional structure of the truncated core of the Saccharomyces cerevisiae pyruvate dehydrogenase complex determined from negative stain and cryoelectron microscopy images*. J Biol Chem, 1992. **267**(34): p. 24769-75.
25. Maeng, C.Y., et al., *Expression, purification, and characterization of the dihydrolipoamide dehydrogenase-binding protein of the pyruvate dehydrogenase complex from Saccharomyces cerevisiae*. Biochemistry, 1994. **33**(46): p. 13801-7.
26. Pronk, J.T., H.Y. Steensma, and J.P. vanDijken, *Pyruvate metabolism in Saccharomyces cerevisiae*. Yeast, 1996. **12**(16): p. 1607-1633.
27. Bowman, S.B., et al., *Positive regulation of the LPD1 gene of Saccharomyces cerevisiae by the HAP2/HAP3/HAP4 activation system*. Mol Gen Genet, 1992. **231**(2): p. 296-303.
28. Gey, U., et al., *Yeast pyruvate dehydrogenase complex is regulated by a concerted activity of two kinases and two phosphatases*. J Biol Chem, 2008. **283**(15): p. 9759-67.

29. Singh, K.K., G.M. Small, and A.S. Lewin, *Alternative topogenic signals in peroxisomal citrate synthase of Saccharomyces cerevisiae*. Mol Cell Biol, 1992. **12**(12): p. 5593-9.
30. Lee, J.G., et al., *Identification of a cryptic N-terminal signal in Saccharomyces cerevisiae peroxisomal citrate synthase that functions in both peroxisomal and mitochondrial targeting*. Journal of Biochemistry, 2000. **128**(6): p. 1059-1072.
31. Hoosein, M.A. and A.S. Lewin, *Derepression of citrate synthase in Saccharomyces cerevisiae may occur at the level of transcription*. Mol Cell Biol, 1984. **4**(2): p. 247-53.
32. Lewin, A.S., V. Hines, and G.M. Small, *Citrate synthase encoded by the CIT2 gene of Saccharomyces cerevisiae is peroxisomal*. Mol Cell Biol, 1990. **10**(4): p. 1399-1405.
33. Graybill, E.R., et al., *Functional comparison of citrate synthase isoforms from S. cerevisiae*. Arch Biochem Biophys, 2007. **465**(1): p. 26-37.
34. Kim, K.S., M.S. Rosenkrantz, and L. Guarente, *Saccharomyces cerevisiae contains two functional citrate synthase genes*. Mol Cell Biol, 1986. **6**(6): p. 1936-42.
35. Rosenkrantz, M., et al., *The Hap2,3,4 Transcriptional Activator Is Required for Derepression of the Yeast Citrate Synthase Gene, Cit1*. Molecular Microbiology, 1994. **13**(1): p. 119-131.
36. Rosenkrantz, M., et al., *Distinct upstream activation regions for glucose-repressed and derepressed expression of the yeast citrate synthase gene CIT1*. Current Genetics, 1994. **25**(3): p. 185-195.
37. Liu, Z.C. and R.A. Butow, *A transcriptional switch in the expression of yeast tricarboxylic acid cycle genes in response to a reduction or loss of respiratory function*. Mol Cell Biol, 1999. **19**(10): p. 6720-6728.
38. Jia, Y.K., et al., *A basic helix-loop-helix-leucine zipper transcription complex in yeast functions in a signaling pathway from mitochondria to the nucleus*. Molecular and Cellular Biology, 1997. **17**(3): p. 1110-1117.
39. Chelstowska, A. and R.A. Butow, *RTG genes in yeast that function in communication between mitochondria and the nucleus are also required for expression of genes encoding peroxisomal proteins*. Journal of Biological Chemistry, 1995. **270**(30): p. 18141-18146.
40. Ferreira, J.R., et al., *Interaction between Rtg2p and Mks1p in the regulation of the RTG pathway of Saccharomyces cerevisiae*. Gene, 2005. **354**: p. 2-8.
41. Liao, X.S., et al., *Intramitochondrial functions regulate nonmitochondrial citrate synthase (CIT2) expression in Saccharomyces cerevisiae*. Mol Cell Biol, 1991. **11**(1): p. 38-46.
42. Kispal, G., et al., *Metabolic studies on citrate synthase mutants of yeast. A change in phenotype following transformation with an inactive enzyme*. Journal of Biological Chemistry, 1989. **264**(19): p. 11204-10.
43. Kispal, G., et al., *Metabolic changes in Saccharomyces cerevisiae strains lacking citrate synthases*. Journal of Biological Chemistry, 1988. **263**(23): p. 11145-9.
44. Velot, C., et al., *Metabolic effects of mislocalized mitochondrial and peroxisomal citrate synthases in yeast Saccharomyces cerevisiae*. Biochemistry, 1999. **38**(49): p. 16195-204.
45. Yoo, H.S., F.S. Genbauffe, and T.G. Cooper, *Identification of the ureidoglycolate hydrolase gene in the DAL gene cluster of Saccharomyces cerevisiae*. Mol Cell Biol, 1985. **5**(9): p. 2279-88.
46. Kunze, M., et al., *Targeting of malate synthase 1 to the peroxisomes of Saccharomyces cerevisiae cells depends on growth on oleic acid medium*. European Journal of Biochemistry, 2002. **269**(3): p. 915-22.
47. Caspary, F., A. Hartig, and H.J. Schuller, *Constitutive and carbon source-responsive promoter elements are involved in the regulated expression of the Saccharomyces cerevisiae malate synthase gene MLS1*. Mol Gen Genet, 1997. **255**(6): p. 619-27.
48. Kratzer, S. and H.J. Schuller, *Transcriptional control of the yeast acetyl-CoA synthetase gene, ACS1, by the positive regulators CAT8 and ADR1 and the pleiotropic repressor UME6*. Mol Microbiol, 1997. **26**(4): p. 631-41.
49. Scholer, A. and H.J. Schuller, *A carbon source-responsive promoter element necessary for activation of the isocitrate lyase gene ICL1 is common to genes of the gluconeogenic pathway in the yeast Saccharomyces cerevisiae*. Mol Cell Biol, 1994. **14**(6): p. 3613-22.
50. Niederacher, D., et al., *Identification of UAS elements and binding proteins necessary for derepression of Saccharomyces cerevisiae fructose-1,6-bisphosphatase*. Current Genetics, 1992. **22**(5): p. 363-70.
51. Proft, M., D. Grzesitza, and K.D. Entian, *Identification and characterization of regulatory elements in the phosphoenolpyruvate carboxykinase gene PCK1 of Saccharomyces cerevisiae*. Mol Gen Genet, 1995. **246**(3): p. 367-73.
52. Satyanarayana, T. and H.P. Klein, *Studies on acetyl-coenzyme A synthetase of yeast: inhibition by long-chain acyl-coenzyme A esters*. Journal of Bacteriology, 1973. **115**(2): p. 600-6.
53. Satyanarayana, T., A.D. Mandel, and H.P. Klein, *Evidence for two immunologically distinct acetyl-coenzyme A synthetase in yeast*. Biochim Biophys Acta, 1974. **341**(2): p. 396-401.
54. Satyanarayana, T. and H.P. Klein, *Studies on the "aerobic" acetyl-coenzyme A synthetase of Saccharomyces cerevisiae: purification,*

- crystallization, and physical properties of the enzyme. Arch Biochem Biophys, 1976. **174**(2): p. 480-90.
55. Van den Berg, M.A. and H.Y. Steensma, *ACS2, a Saccharomyces cerevisiae gene encoding acetyl-coenzyme A synthetase, essential for growth on glucose*. Eur J Biochem, 1995. **231**(3): p. 704-13.
 56. Kumar, A., et al., *Subcellular localization of the yeast proteome*. Genes Dev, 2002. **16**(6): p. 707-19.
 57. Huh, W.K., et al., *Global analysis of protein localization in budding yeast*. Nature, 2003. **425**(6959): p. 686-91.
 58. van den Berg, M.A., et al., *The two acetyl-coenzyme A synthetases of Saccharomyces cerevisiae differ with respect to kinetic properties and transcriptional regulation*. J Biol Chem, 1996. **271**(46): p. 28953-9.
 59. Devirgilio, C., et al., *Cloning and disruption of a gene required for growth on acetate but not on ethanol: the acetyl-coenzyme A synthetase gene of Saccharomyces cerevisiae*. Yeast, 1992. **8**(12): p. 1043-1051.
 60. Kratzer, S. and H.J. Schuller, *Carbon source-dependent regulation of the acetyl-coenzyme A synthetase-encoding gene ACS1 from Saccharomyces cerevisiae*. Gene, 1995. **161**(1): p. 75-9.
 61. Hiesinger, M., C. Wagner, and H.J. Schuller, *The acetyl-CoA synthetase gene ACS2 of the yeast Saccharomyces cerevisiae is coregulated with structural genes of fatty acid biosynthesis by the transcriptional activators Ino2p and Ino4p*. FEBS Lett, 1997. **415**(1): p. 16-20.
 62. Schuller, H.J., et al., *Coordinate genetic control of yeast fatty acid synthase genes FAS1 and FAS2 by an upstream activation site common to genes involved in membrane lipid biosynthesis*. EMBO J, 1992. **11**(1): p. 107-14.
 63. Starai, V.J., et al., *Sir2-dependent activation of acetyl-CoA synthetase by deacetylation of active lysine*. Science, 2002. **298**(5602): p. 2390-2.
 64. Starai, V.J. and J.C. Escalante-Semerena, *Acetyl-coenzyme A synthetase (AMP forming)*. Cell Mol Life Sci, 2004. **61**(16): p. 2020-30.
 65. Starai, V.J., et al., *A link between transcription and intermediary metabolism: a role for Sir2 in the control of acetyl-coenzyme A synthetase*. Current Opinion in Microbiology, 2004. **7**(2): p. 115-119.
 66. van Roermund, C.W., et al., *Fatty acid metabolism in Saccharomyces cerevisiae*. Cell Mol Life Sci, 2003. **60**(9): p. 1838-51.
 67. Al-Feel, W., S.S. Chirala, and S.J. Wakil, *Cloning of the yeast FAS3 gene and primary structure of yeast acetyl-CoA carboxylase*. Proc Natl Acad Sci U S A, 1992. **89**(10): p. 4534-8.
 68. Hoja, U., et al., *HFA1 encoding an organelle-specific acetyl-CoA carboxylase controls mitochondrial fatty acid synthesis in Saccharomyces cerevisiae*. Journal of Biological Chemistry, 2004. **279**(21): p. 21779-21786.
 69. Hasslacher, M., et al., *Acetyl-CoA carboxylase from yeast is an essential enzyme and is regulated by factors that control phospholipid metabolism*. Journal of Biological Chemistry, 1993. **268**(15): p. 10946-10952.
 70. Tehlivets, O., K. Scheuringer, and S.D. Kohlwein, *Fatty acid synthesis and elongation in yeast*. Biochimica Et Biophysica Acta-Molecular and Cell Biology of Lipids, 2007. **1771**(3): p. 255-270.
 71. Witters, L.A. and T.D. Watts, *Yeast acetyl-CoA carboxylase: in vitro phosphorylation by mammalian and yeast protein kinases*. Biochem Biophys Res Commun, 1990. **169**(2): p. 369-76.
 72. Woods, A., et al., *Yeast SNF1 is functionally related to mammalian AMP-activated protein kinase and regulates acetyl-CoA carboxylase in vivo*. J Biol Chem, 1994. **269**(30): p. 19509-15.
 73. Shi, S., et al., *Improving production of malonyl coenzyme A-derived metabolites by abolishing Snf1-dependent regulation of Acc1*. MBio, 2014. **5**(3): p. e01130-14.
 74. Hofbauer, H.F., et al., *Regulation of Gene Expression through a Transcriptional Repressor that Senses Acyl-Chain Length in Membrane Phospholipids*. Developmental Cell, 2014. **29**(6): p. 729-739.
 75. Hiser, L., M.E. Basson, and J. Rine, *ERG10 from Saccharomyces cerevisiae encodes acetoacetyl-CoA thiolase*. Journal of Biological Chemistry, 1994. **269**(50): p. 31383-9.
 76. van Roermund, C.W., et al., *The membrane of peroxisomes in Saccharomyces cerevisiae is impermeable to NAD(H) and acetyl-CoA under in vivo conditions*. EMBO J, 1995. **14**(14): p. 3480-6.
 77. Strijbis, K. and B. Distel, *Intracellular acetyl unit transport in fungal carbon metabolism*. Eukaryot Cell, 2010. **9**(12): p. 1809-15.
 78. Flikweert, M.T., et al., *Growth requirements of pyruvate-decarboxylase-negative Saccharomyces cerevisiae*. FEMS Microbiol Lett, 1999. **174**(1): p. 73-9.
 79. van Roermund, C.W., et al., *Molecular characterization of carnitine-dependent transport of acetyl-CoA from peroxisomes to mitochondria in Saccharomyces cerevisiae and identification of a plasma membrane carnitine transporter, Agp2p*. EMBO J, 1999. **18**(21): p. 5843-52.
 80. Li, Z.Y., E. Haase, and M. Brendel, *Hyper-resistance to nitrogen mustard in Saccharomyces cerevisiae is caused by defective choline transport*. Curr Genet, 1991. **19**(6): p. 423-7.
 81. Aouida, M., et al., *Agp2, a member of the yeast amino acid permease family, positively regulates polyamine transport at the transcriptional level*. PLoS One, 2013. **8**(6): p. e65717.
 82. Elgersma, Y., et al., *Peroxisomal and mitochondrial carnitine acetyltransferases of Saccharomyces*

- cerevisiae* are encoded by a single gene. EMBO J, 1995. **14**(14): p. 3472-3479.
83. Schmalix, W. and W. Bandlow, *The ethanol-inducible YAT1 gene from yeast encodes a presumptive mitochondrial outer carnitine acetyltransferase*. Journal of Biological Chemistry, 1993. **268**(36): p. 27428-27439.
 84. Swiegers, J.H., et al., *Carnitine-dependent metabolic activities in Saccharomyces cerevisiae: three carnitine acetyltransferases are essential in a carnitine-dependent strain*. Yeast, 2001. **18**(7): p. 585-95.
 85. Palmieri, L., et al., *Identification of the mitochondrial carnitine carrier in Saccharomyces cerevisiae*. Febs Letters, 1999. **462**(3): p. 472-476.
 86. Jones, J.D. and C.D. O'Connor, *Protein acetylation in prokaryotes*. Proteomics, 2011. **11**(15): p. 3012-22.
 87. Soppa, J., *Protein acetylation in archaea, bacteria, and eukaryotes*. Archaea, 2010. **2010**.
 88. Kurdistani, S.K., S. Tavazoie, and M. Grunstein, *Mapping global histone acetylation patterns to gene expression*. Cell, 2004. **117**(6): p. 721-33.
 89. Spange, S., et al., *Acetylation of non-histone proteins modulates cellular signalling at multiple levels*. International Journal of Biochemistry & Cell Biology, 2009. **41**(1): p. 185-198.
 90. Yang, X.J. and E. Seto, *Lysine acetylation: Codified crosstalk with other posttranslational modifications*. Molecular Cell, 2008. **31**(4): p. 449-461.
 91. Glozak, M.A., et al., *Acetylation and deacetylation of non-histone proteins*. Gene, 2005. **363**: p. 15-23.
 92. Galdieri, L. and A. Vancura, *Acetyl-CoA carboxylase regulates global histone acetylation*. Journal of Biological Chemistry, 2012. **287**(28): p. 23865-76.
 93. Cai, L. and B.P. Tu, *Acetyl-CoA drives the transcriptional growth program in yeast*. Cell Cycle, 2011. **10**(18): p. 3045-6.
 94. Shi, L. and B.P. Tu, *Acetyl-CoA induces transcription of the key G1 cyclin CLN3 to promote entry into the cell division cycle in Saccharomyces cerevisiae*. Proceedings of the National Academy of Sciences of the United States of America, 2013. **110**(18): p. 7318-7323.
 95. Cai, L. and B.P. Tu, *On acetyl-CoA as a gauge of cellular metabolic state*. Cold Spring Harb Symp Quant Biol, 2011. **76**: p. 195-202.
 96. Leskovac, V., S. Trivic, and D. Pericin, *The three zinc-containing alcohol dehydrogenases from baker's yeast, Saccharomyces cerevisiae*. FEMS Yeast Res, 2002. **2**(4): p. 481-94.
 97. Schaaff, I., et al., *A deletion of the PDC1 gene for pyruvate decarboxylase of yeast causes a different phenotype than previously isolated point mutations*. Curr Genet, 1989. **15**(2): p. 75-81.
 98. Hohmann, S. and H. Cederberg, *Autoregulation may control the expression of yeast pyruvate decarboxylase structural genes PDC1 and PDC5*. Eur J Biochem, 1990. **188**(3): p. 615-21.
 99. Hohmann, S., *Characterization of PDC6, a third structural gene for pyruvate decarboxylase in Saccharomyces cerevisiae*. Journal of Bacteriology, 1991. **173**(24): p. 7963-9.
 100. Schmitt, H.D. and F.K. Zimmermann, *Genetic analysis of the pyruvate decarboxylase reaction in yeast glycolysis*. Journal of Bacteriology, 1982. **151**(3): p. 1146-52.
 101. Seeboth, P.G., K. Bohnsack, and C.P. Hollenberg, *pdC1(0) mutants of Saccharomyces cerevisiae give evidence for an additional structural PDC gene: cloning of PDC5, a gene homologous to PDC1*. Journal of Bacteriology, 1990. **172**(2): p. 678-85.
 102. Muller, E.H., et al., *Thiamine repression and pyruvate decarboxylase autoregulation independently control the expression of the Saccharomyces cerevisiae PDC5 gene*. FEBS Lett, 1999. **449**(2-3): p. 245-50.
 103. Hohmann, S., *PDC6, a weakly expressed pyruvate decarboxylase gene from yeast, is activated when fused spontaneously under the control of the PDC1 promoter*. Curr Genet, 1991. **20**(5): p. 373-8.
 104. Flikweert, M.T., et al., *Pyruvate decarboxylase: an indispensable enzyme for growth of Saccharomyces cerevisiae on glucose*. Yeast, 1996. **12**(3): p. 247-57.
 105. Flikweert, M.T., J.P. van Dijken, and J.T. Pronk, *Metabolic responses of pyruvate decarboxylase-negative Saccharomyces cerevisiae to glucose excess*. Appl Environ Microbiol, 1997. **63**(9): p. 3399-404.
 106. van Maris, A.J., et al., *Overproduction of threonine aldolase circumvents the biosynthetic role of pyruvate decarboxylase in glucose-limited chemostat cultures of Saccharomyces cerevisiae*. Appl Environ Microbiol, 2003. **69**(4): p. 2094-9.
 107. van Maris, A.J., et al., *Directed evolution of pyruvate decarboxylase-negative Saccharomyces cerevisiae, yielding a C2-independent, glucose-tolerant, and pyruvate-hyperproducing yeast*. Appl Environ Microbiol, 2004. **70**(1): p. 159-66.
 108. Oud, B., et al., *An internal deletion in MTH1 enables growth on glucose of pyruvate-decarboxylase negative, non-fermentative Saccharomyces cerevisiae*. Microb Cell Fact, 2012. **11**(1): p. 131.
 109. Lakshmanan, J., A.L. Mosley, and S. Ozcan, *Repression of transcription by Rgt1 in the absence of glucose requires Std1 and Mth1*. Curr Genet, 2003. **44**(1): p. 19-25.
 110. Polish, J.A., J.H. Kim, and M. Johnston, *How the Rgt1 transcription factor of Saccharomyces cerevisiae is repressed by glucose*. Genetics, 2005. **169**(2): p. 583-594.
 111. Gamo, F.J., M.J. Lafuente, and C. Gancedo, *The mutation DGT1-1 decreases glucose transport and alleviates carbon catabolite repression in*

- Saccharomyces cerevisiae*. Journal of Bacteriology, 1994. **176**(24): p. 7423-9.
112. Blazquez, M.A., F.J. Gamo, and C. Gancedo, *A mutation affecting carbon catabolite repression suppresses growth defects in pyruvate carboxylase mutants from Saccharomyces cerevisiae*. FEBS Lett, 1995. **377**(2): p. 197-200.
 113. Lafuente, M.J., et al., *Mth1 receives the signal given by the glucose sensors Snf3 and Rgt2 in Saccharomyces cerevisiae*. Mol Microbiol, 2000. **35**(1): p. 161-72.
 114. Schulte, F., et al., *The HTR1 gene is a dominant negative mutant allele of MTH1 and blocks Snf3- and Rgt2-dependent glucose signaling in yeast*. Journal of Bacteriology, 2000. **182**(2): p. 540-542.
 115. Ozcan, S., et al., *Glucose uptake and catabolite repression in dominant HTR1 mutants of Saccharomyces cerevisiae*. Journal of Bacteriology, 1993. **175**(17): p. 5520-8.
 116. Moriya, H. and M. Johnston, *Glucose sensing and signaling in Saccharomyces cerevisiae through the Rgt2 glucose sensor and casein kinase I*. Proceedings of the National Academy of Sciences of the United States of America, 2004. **101**(6): p. 1572-1577.
 117. Conrad, T.M., N.E. Lewis, and B.O. Palsson, *Microbial laboratory evolution in the era of genome-scale science*. Mol Syst Biol, 2011. **7**: p. 509.
 118. Bailey, J.E., et al., *Strategies and challenges in metabolic engineering*. Ann N Y Acad Sci, 1990. **589**: p. 1-15.
 119. Nielsen, J., *Metabolic engineering*. Appl Microbiol Biotechnol, 2001. **55**(3): p. 263-83.
 120. Jensen, M.K. and J.D. Keasling, *Recent applications of synthetic biology tools for yeast metabolic engineering*. FEMS Yeast Res, 2014.
 121. Krivoruchko, A., V. Siewers, and J. Nielsen, *Opportunities for yeast metabolic engineering: Lessons from synthetic biology*. Biotechnol J, 2011. **6**(3): p. 262-76.
 122. Nielsen, J. and J.D. Keasling, *Synergies between synthetic biology and metabolic engineering*. Nat Biotechnol, 2011. **29**(8): p. 693-5.
 123. Oud, B., et al., *Genome-wide analytical approaches for reverse metabolic engineering of industrially relevant phenotypes in yeast*. FEMS Yeast Res, 2012. **12**(2): p. 183-96.
 124. Bailey, J.E., et al., *Inverse metabolic engineering: A strategy for directed genetic engineering of useful phenotypes*. Biotechnol Bioeng, 1996. **52**(1): p. 109-21.
 125. Bro, C., et al., *Improvement of galactose uptake in Saccharomyces cerevisiae through overexpression of phosphoglucosmutase: example of transcript analysis as a tool in inverse metabolic engineering*. Appl Environ Microbiol, 2005. **71**(11): p. 6465-72.
 126. Hong, K.K. and J. Nielsen, *Recovery of phenotypes obtained by adaptive evolution through inverse metabolic engineering*. Appl Environ Microbiol, 2012. **78**(21): p. 7579-86.
 127. Caspeta, L., et al., *Biofuels. Altered sterol composition renders yeast thermotolerant*. Science, 2014. **346**(6205): p. 75-8.
 128. Portnoy, V.A., D. Bezdán, and K. Zengler, *Adaptive laboratory evolution--harnessing the power of biology for metabolic engineering*. Curr Opin Biotechnol, 2011. **22**(4): p. 590-4.
 129. van Maris, A.J.A., et al., *Directed Evolution of Pyruvate Decarboxylase-Negative Saccharomyces cerevisiae, Yielding a C2-Independent, Glucose-Tolerant, and Pyruvate-Hyperproducing Yeast*. Appl. Environ. Microbiol., 2004. **70**(1): p. 159-166.
 130. Österlund, T., et al., *Mapping condition-dependent regulation of metabolism in yeast through genome-scale modeling*. BMC Systems Biology, 2013. **7**.
 131. Lee, F.J.S., L.W. Lin, and J.A. Smith, *Purification and characterization of an acetyl-CoA hydrolase from Saccharomyces cerevisiae*. European Journal of Biochemistry, 1989. **184**(1): p. 21-28.
 132. Lee, F.J.S., L.W. Lin, and J.A. Smith, *A glucose-repressible gene encodes acetyl-CoA hydrolase from Saccharomyces cerevisiae*. J. Biol. Chem., 1990. **265**(13): p. 7413-7418.
 133. Lee, F.J.S., L.W. Lin, and J.A. Smith, *Acetyl-CoA hydrolase involved in acetate utilization in Saccharomyces cerevisiae*. Biochimica et Biophysica Acta - Protein Structure and Molecular Enzymology, 1996. **1297**(1): p. 105-109.
 134. Buu, L.M., Y.C. Chen, and F.J.S. Lee, *Functional characterization and localization of acetyl-CoA hydrolase, Ach1p, in Saccharomyces cerevisiae*. J. Biol. Chem., 2003. **278**(19): p. 17203-17209.
 135. Gergely, J., P. Hele, and C.V. Ramakrishnan, *Succinyl and acetyl coenzyme a deacylases*. The Journal of biological chemistry, 1952. **198**(1): p. 324-334.
 136. Knowles, S.E., et al., *Production and utilization of acetate in mammals*. Biochemical Journal, 1974. **142**(2): p. 401-411.
 137. Fleck, C.B. and M. Brock, *Re-characterisation of Saccharomyces cerevisiae Ach1p: Fungal CoA-transferases are involved in acetic acid detoxification*. Fungal Genetics and Biology, 2009. **46**(6-7): p. 473-485.
 138. Entian, K.-D. and P. Kötter, *25 Yeast Genetic Strain and Plasmid Collections*, in *Methods in Microbiology*, S. Ian and J.R.S. Michael, Editors. 2007, Academic Press. p. 629-666.
 139. Chen, Y., et al., *Enhancing the copy number of episomal plasmids in Saccharomyces cerevisiae for improved protein production*. FEMS Yeast Res, 2012. **12**(5): p. 598-607.
 140. Halestrap, A.P., *The mitochondrial pyruvate carrier. Kinetics and specificity for substrates and inhibitors*. Biochemical Journal, 1975. **148**(1): p. 85-96.

141. Bricker, D.K., et al., *A mitochondrial pyruvate carrier required for pyruvate uptake in yeast, Drosophila, and humans*. *Science*, 2012. **336**(6090): p. 96-100.
142. Rivière, L., et al., *Acetate produced in the mitochondrion is the essential precursor for lipid biosynthesis in procyclic trypanosomes*. *Proceedings of the National Academy of Sciences*, 2009. **106**(31): p. 12694-12699.
143. Erdeniz, N., U.H. Mortensen, and R. Rothstein, *Cloning-free PCR-based allele replacement methods*. *Genome Research*, 1997. **7**(12): p. 1174-1183.
144. Gietz, R.D. and R.A. Woods, *Transformation of yeast by lithium acetate/single-stranded carrier DNA/polyethylene glycol method*. *Methods Enzymol*, 2002. **350**: p. 87-96.
145. Guldener, U., et al., *A new efficient gene disruption cassette for repeated use in budding yeast*. *Nucleic Acids Res*, 1996. **24**(13): p. 2519-24.
146. McKenna, A., et al., *The Genome Analysis Toolkit: a MapReduce framework for analyzing next-generation DNA sequencing data*. *Genome Research*, 2010. **20**(9): p. 1297-303.
147. Ozcan, S. and M. Johnston, *Three different regulatory mechanisms enable yeast hexose transporter (HXT) genes to be induced by different levels of glucose*. *Mol Cell Biol*, 1995. **15**(3): p. 1564-72.
148. Gancedo, J.M., *The early steps of glucose signalling in yeast*. *Fems Microbiology Reviews*, 2008. **32**(4): p. 673-704.
149. Ruiz-Roig, C., et al., *The Rpd3L HDAC complex is essential for the heat stress response in yeast*. *Mol Microbiol*, 2010. **76**(4): p. 1049-62.
150. Knott, S.R., et al., *Genome-wide replication profiles indicate an expansive role for Rpd3L in regulating replication initiation timing or efficiency, and reveal genomic loci of Rpd3 function in Saccharomyces cerevisiae*. *Genes Dev*, 2009. **23**(9): p. 1077-90.
151. Yi, C., et al., *Function and molecular mechanism of acetylation in autophagy regulation*. *Science*, 2012. **336**(6080): p. 474-7.
152. Teste, M.A., et al., *Validation of reference genes for quantitative expression analysis by real-time RT-PCR in Saccharomyces cerevisiae*. *BMC Mol Biol*, 2009. **10**: p. 99.
153. Edgar, R.C., *MUSCLE: multiple sequence alignment with high accuracy and high throughput*. *Nucleic Acids Res*, 2004. **32**(5): p. 1792-7.
154. Kiefer, F., et al., *The SWISS-MODEL Repository and associated resources*. *Nucleic Acids Res*, 2009. **37**(Database issue): p. D387-92.
155. Cole, C., J.D. Barber, and G.J. Barton, *The Jpred 3 secondary structure prediction server*. *Nucleic Acids Research*, 2008. **36**: p. W197-W201.
156. Roy, A., A. Kucukural, and Y. Zhang, *I-TASSER: a unified platform for automated protein structure and function prediction*. *Nat Protoc*, 2010. **5**(4): p. 725-38.
157. Deng, D., et al., *Crystal structure of the human glucose transporter GLUT1*. *Nature*, 2014. **510**(7503): p. 121-5.
158. Reifemberger, E., E. Boles, and M. Ciriacy, *Kinetic characterization of individual hexose transporters of Saccharomyces cerevisiae and their relation to the triggering mechanisms of glucose repression*. *Eur J Biochem*, 1997. **245**(2): p. 324-33.
159. Ozcan, S. and M. Johnston, *Function and regulation of yeast hexose transporters*. *Microbiol Mol Biol Rev*, 1999. **63**(3): p. 554-69.
160. Kurdistani, S.K. and M. Grunstein, *Histone acetylation and deacetylation in yeast*. *Nat Rev Mol Cell Biol*, 2003. **4**(4): p. 276-84.
161. Knappe, J. and G. Sawers, *A radical-chemical route to acetyl-CoA: the anaerobically induced pyruvate formate-lyase system of Escherichia coli*. *FEMS Microbiol Rev*, 1990. **6**(4): p. 383-98.
162. Sawers, G. and G. Watson, *A glycyl radical solution: oxygen-dependent interconversion of pyruvate formate-lyase*. *Mol Microbiol*, 1998. **29**(4): p. 945-54.
163. Frey, M., et al., *Adenosylmethionine-dependent synthesis of the glycyl radical in pyruvate formate-lyase by abstraction of the glycine C-2 pro-S hydrogen atom*. *Studies of [2H]glycine-substituted enzyme and peptides homologous to the glycine 734 site*. *J Biol Chem*, 1994. **269**(17): p. 12432-7.
164. Waks, Z. and P.A. Silver, *Engineering a synthetic dual-organism system for hydrogen production*. *Appl Environ Microbiol*, 2009. **75**(7): p. 1867-75.
165. Wagner, A.F., et al., *The free radical in pyruvate formate-lyase is located on glycine-734*. *Proc Natl Acad Sci U S A*, 1992. **89**(3): p. 996-1000.
166. Sancho, J., *Flavodoxins: sequence, folding, binding, function and beyond*. *Cell Mol Life Sci*, 2006. **63**(7-8): p. 855-64.
167. Osborne, C., L.M. Chen, and R.G. Matthews, *Isolation, cloning, mapping, and nucleotide sequencing of the gene encoding flavodoxin in Escherichia coli*. *Journal of Bacteriology*, 1991. **173**(5): p. 1729-37.
168. Knoell, H.E. and J. Knappe, *Escherichia coli ferredoxin, an iron-sulfur protein of the adrenodoxin type*. *Eur J Biochem*, 1974. **50**(1): p. 245-52.
169. Overkamp, K.M., et al., *Functional analysis of structural genes for NAD(+)-dependent formate dehydrogenase in Saccharomyces cerevisiae*. *Yeast*, 2002. **19**(6): p. 509-20.